

## EDITORIAL BOARD

**Tudor BÎNZAR – Editor in Chief**

**Liviu CĂDARIU**

Executive Editor for Mathematics  
liviu.cadariu-brailoiu@upt.ro

**Dușan POPOV**

Executive Editor for Physics  
dusan.popov@upt.ro

**Camelia ARIEȘANU** - Department of Mathematics, Politehnica University Timisoara

**Nicolae M. AVRAM** - Faculty of Physics, West University of Timisoara

**Titu BÂNZARU** - Department of Mathematics, Politehnica University Timisoara

**Nicolae BOJA** - Department of Mathematics, Politehnica University Timisoara

**Constantin CORDUNEANU** - University of Texas at Arlington, U.S.A.

**Emeric DEUTSCH** - Politechnic University-Brooklyn, New York, U.S.A.

**Sever S. DRAGOMIR** - School of Engineering&Science, Victoria University of Melbourne, Australia

**Mirela FETEA** - Department of Physics, University of Richmond, U.S.A.

**Marian GRECONICI** - Depart. of Physical Fundamentals of Engineering, Politehnica University Timisoara

**Pașc GĂVRUȚA** - Department of Mathematics, Politehnica University Timisoara

**Jovo JARIĆ** - Faculty of Mathematics, University of Belgrade, Serbia

**Maria JIVULESCU** - Department of Mathematics, Politehnica University Timisoara

**Darko KAPOR** - Institute of Physics, University of Novi Sad, Serbia

**Octavian LIPOVAN** - Department of Mathematics, Politehnica University Timisoara

**Dragoljub Lj. MIRJANIĆ** - Academy of Science and Art of the Republic of Srpska, Bosnia and Herzegovina

**Ioan MUȘCUTARIU** - Faculty of Physics, West University of Timisoara

**Romeo NEGREA** - Department of Mathematics, Politehnica University Timisoara

**Emilia PETRIȘOR** - Department of Mathematics, Politehnica University Timisoara

**Mohsen RAZZAGHI** - Dep. of Math. and Statistics, Mississippi State Univ., U.S.A.

**Gheorghe ȚIGAN** - Department of Mathematics, Politehnica University Timisoara

**Ioan ZAHARIE** - Dept. of Physical Fundamentals of Engineering, Politehnica University Timisoara

Please consider, when preparing the manuscript, the *Instructions for the Authors* at the end of each issue. Orders, exchange for other journals, manuscripts and all correspondences concerning off prints should be sent to the Executive Editors or to the editorial secretaries at the address:

Politehnica University Timisoara  
Department of Mathematics  
Victoriei Square, No. 2  
300006–Timisoara, Romania  
Tel.: +40-256-403099  
Fax: +40-(0)256-403109

Politehnica University Timisoara  
Department of Physical Fundamentals  
of Engineering  
B-dul. Vasile Parvan, No. 2  
300223–Timisoara, Romania  
Tel.: +40-256-403391  
Fax: +40-(0)256-403392

## Contents

<b>Constantin Corduneanu</b> – In Memoriam . . . . .	4
<b>C. Pop, I. R. Iosif</b> – Stability Problems and Numerical Integration on the Poincaré Lie Group . . . . .	5
<b>C. Lăzureanu, C. Petrișor</b> – On the Dynamics of a Hamilton-Poisson System . . . . .	14
<b>I. R. Iosif</b> – Some Properties of Cortical Bones . . . . .	29
<b>S. Lugojan, L. Ciurdariu</b> – A generalization of Young’s Theorem and some applications . . . . .	49
<b>L. Ciurdariu, S. Lugojan</b> – Application of the non-convex Young’s Inequality in Hilbert Space . . . . .	57
<b>E. Vasilache</b> — Some Concepts of Fractional Differential Calculus using MATLAB . . . . .	62

## In Memoriam - Constantin CORDUNEANU

July 26, 1928 - December 26, 2018

Last December **Professor Constantin CORDUNEANU** left us at the age of 90. He was a member of the Editorial Board of the Scientific Bulletin of Politehnica University of Timisoara, Transactions on Mathematics and Physics since 2002.

**Constantin Corduneanu** was born in the Romanian village of Potangeni, Iași county. In 1951 he graduated the University of Iași. Four years later he obtained his PhD degree in Mathematics having Professor Ilie Popa as PhD Advisor and professors Miron Nicolescu, Grigore C. Moisil and Adolf Haimovici as referees.

Between 1949 and 1977 he was assistant, lecturer, associated professor, then professor at the "Alexandru Ioan Cuza" University of Iași, Faculty of Mathematics. He was appointed Dean of the Faculty of Mathematics (1968-1972) and Rector of the University (1966-1968). He became a member of the Romanian Academy in 1974.

**Constantin Corduneanu** left the country in 1978 to become a professor at the University of Texas at Arlington, USA. He published more than 200 books and scientific articles from various research areas such as differential equations, stability theory or theory of oscillating movements and waves. Dr. Corduneanu taught for over 4000 Romanian and 3000 American Students and guided over 20 PhD students.

**Dr. Corduneanu** was the first author from Iași whose book was translated in USA (Almost Periodic Functions, John Wiley, New York, 1968, Chelsea, 1989). Other important books containing the lectures he taught in Romania or in USA were published at prestigious publishing houses: *Integral Equations and Stability of Feedback Systems* (New York, 1973), *Integral Equations and Applications* (Cambridge University Press, 1991 and 2008), *Functional Equations with Causal Operators* (Taylor and Francis, London, 2002), *Almost periodic oscillations and waves* (Boston, New York, 2009).

**Dr. Corduneanu** was a member of the Editorial Boards of several Journals including the Scientific Annals of "Alexandru Ioan Cuza" University of Iași, Mathematics Transitions, Revue Roumaine de Mathématiques Pures et Appliquées, Journal of Integral Equations and Applications, Differential and Integral Equations, Nonlinear Analysis - TMA and in his last years he has collaborated with nine mathematical journals from Romania, China, Ukraine, Israel and South Korea.

**Professor Corduneanu** was a recipient of the Ministry of Education Prize in 1963, the "Gheorghe Lazăr" Prize of Romanian Academy in 1965, the Distinguished Research Award of the University of Texas at Arlington, USA in 1991 and The Medal of Merit of the Czech Mathematical Society in 2001.

Editors - The Scientific Bulletin of  
Politehnica University of Timisoara

## STABILITY PROBLEMS AND NUMERICAL INTEGRATION ON THE POINCARÉ LIE GROUP

Camelia POP, Ramona Ioana IOSIF

### Abstract

An underactuated drift-free left-invariant control system on the Lie group  $ISO(3, 1)$  is analyzed. <sup>1</sup>

Keywords and phrases: *spectral stability, Lie group*

## 1 Introduction

The Poincaré group  $ISO(3, 1)$  was first defined by Minkowski (1908) as the group of Minkowski space-time isometries. It can be written as a semi-direct product of the Lorentz group  $SO(3,1)$  with the four-dimensional translation group  $R^4$ . Due to its big importance in quantum theory of fields, we are interested to study an optimal control problem on this Lie group. The interest in such problems arise from their deep applications in engineering (spacecraft dynamics, sub-aquatic dynamics, the tower control problem), in chemistry (molecular motion control) or physics (quantum theory).

## 2 An optimal control problem on the Poincaré Lie group

Let us consider  $\{J_i, K_i, P_i, H\}_{(1=i,j=3)}$  the usual generators of spatial rotations, boosts, space translations, and time translation respectively, of the Poincaré inhomogeneous Lie algebra  $iso(3, 1)$ ; the nonzero brackets are given by:

$$[J_i, J_j] = \varepsilon_{ijk} J_k; [J_i, P_j] = \varepsilon_{ijk} P_k; [J_i, K_j] = \varepsilon_{ijk} K_k;$$

$$[H, K_j] = P_j; [K_i, K_j] = -\varepsilon_{ijk} J_k; [P_i, K_i] = H.$$

---

<sup>1</sup>MSC(2010): 34A26, 34H05, 34M45, 35A24, 37C10, 49J15, 49K15, 93C15

A general left invariant drift free control system on the Poincaré Lie algebra  $iso(3, 1)$  with fewer controls than state variables can be written in the following form:

$$\dot{X} = X\left(\sum_{i=1}^m u_i A_i\right),$$

where  $X \in ISO(3, 1)$ , the functions  $u_i$  are the control inputs, and  $m < 10$ . In all that follows, we shall concentrate to the following left-invariant, drift-free control system on  $ISO(3, 1)$  with 4 controls:

$$\dot{X} = X(u_1 J_1 + u_2 K_1 u_3 K_2 + u_4 H). \quad (1)$$

**Theorem 2.1** *The system (1) is controllable.*

**Proof:** Since the span of the set of Lie brackets generated by  $J_1, K_1, K_2, H$  coincides with  $iso(3, 1)$ , the Proposition is a consequence of a result due to Jur-djevic and Sussman, see [6].

Let  $C$  be the cost function given by:

$$C(u_1, u_2, u_3, u_4) = \frac{1}{2} \int_0^{t_f} [u_1^2(t) + u_2^2(t) + u_3^2(t) + u_4^2(t)] dt.$$

The controls that minimize  $C$  and steer the system (1) from the initial state  $X = X_0$  at  $t = 0$  to the final state  $X = X_f$  at  $t = t_f$  are giving by the solutions of the following differential equations:

$$\left\{ \begin{array}{l} j_1' = k_2 k_3 \\ j_2' = -j_1 j_3 - k_1 k_3 \\ j_3' = j_1 j_2 \\ k_1' = -k_2 j_3 + h p_1 \\ k_2' = -k_3 j_1 + k_1 j_3 + h p_2 \\ k_3' = 2j_1 k_2 - j_2 k_1 + h p_3 \\ p_1' = -h k_1 \\ p_2' = -j_1 p_3 - h k_2 \\ p_3' = j_1 p_2 \\ h' = k_1 p_1 - p_2 k_2 \end{array} \right. \quad (2)$$

The system is obtained by applying Krishnaprasad's theorem (see [7]) to the optimal Hamiltonian given by:

$$H_{opt} = \frac{1}{2}(j_1^2 + k_1^2 + k_2^2 + h^2).$$

**Theorem 2.2** *The dynamics (2) has the following Poisson realization:*

$$(iso(3, 1), \Pi_-, H),$$

where:

$$\Pi_- = \begin{pmatrix} 0 & j_3 & -j_2 & 0 & k_3 & -k_2 & 0 & p_3 & -p_2 & 0 \\ -j_3 & 0 & j_1 & -k_3 & 0 & k_1 & -p_3 & 0 & p_1 & 0 \\ j_2 & -j_1 & 0 & k_2 & -k_1 & 0 & p_2 & -p_1 & 0 & 0 \\ 0 & k_3 & -k_2 & 0 & -j_3 & j_2 & h & 0 & 0 & p_1 \\ -k_3 & 0 & k_1 & j_3 & 0 & -j_1 & 0 & h & 0 & p_2 \\ j_2 & -k_1 & 0 & -j_2 & j_1 & 0 & 0 & 0 & h & p_3 \\ 0 & p_3 & -p_2 & -h & 0 & 0 & 0 & 0 & 0 & 0 \\ -p_3 & 0 & p_1 & 0 & -h & 0 & 0 & 0 & 0 & 0 \\ p_2 & -p_1 & 0 & 0 & 0 & -h & 0 & 0 & 0 & 0 \\ 0 & 0 & 0 & -p_1 & -p_2 & -p_3 & 0 & 0 & 0 & 0 \end{pmatrix} \quad (3)$$

is the minus-Lie-Poisson structure on  $iso(3, 1)$ , and

$$H = \frac{1}{2}(j_1^2 + k_1^2 + k_2^2 + h^2)$$

is the Hamiltonian function.

**Proof:** Indeed, it is not hard to see that the dynamics (2) can be written as

$$\begin{pmatrix} j_1' & j_2' & j_3' & k_1' & k_2' & k_3' & p_1' & p_2' & p_3' & h' \end{pmatrix}^t = \Pi_- \cdot H$$

and  $\Pi_-$  is the minus-Lie-Poisson structure on  $iso(3, 1)$ .

**Corollary 2.1** *The Lie-Poisson structure  $\Pi_-$  admits two linear independent Casimir operators:*

$$C_1 = \frac{1}{2}(p_1^2 + p_2^2 + p_3^2 - h^2), \quad (4)$$

and

$$C_2 = (-hj_3 - p_1k_2 + p_2k_1)^2 + (hk_2 - p_1k_3 + p_3k_1)^2 + (-hj_1 - p_2k_3 + p_3k_2)^2 - (p_3j_3 + p_1j_1 + p_2j_2)^2. \quad (5)$$

### 3 Stability

The goal of this section is to analyze the spectral stability of the equilibrium states of the dynamics (2):

$$e_1^{MNPQRS} = (0, M, N, 0, 0, P, Q, R, S, 0), e_2^{MNPQ} = (0, 0, 0, M, N, 0, P, -\frac{MP}{N}, Q, 0),$$

$$e_3^{MNPQ} = (0, M, 0, 0, N, 0, P, 0, Q, 0), e_4^{MNPQ} = (0, 0, M, 0, 0, N, P, 0, Q, 0),$$

$$e_5^{MNP} = (0, 0, 0, M, 0, 0, 0, N, P, 0), e_6^{MN} = (M, 0, 0, N, 0, 0, 0, 0, 0, 0),$$

$$e_7^{MN} = (M, 0, 0, 0, 0, 0, N, 0, 0, 0), e_8^{MN} = (-\frac{M}{\sqrt{2}}, 0, 0, 0, N, 0, 0, 0, \sqrt{2}, M),$$

$$e_9^{MN} = (M, 0, 0, 0, 0, 0, 0, 0, 0, N), e_{10}^{MNPQ} = (0, M, N, 0, 0, P, 0, 0, 0, Q).$$

**Theorem 3.1** (i) *The equilibrium states  $e_1^{MNPQRS}$  are spectrally stable iff  $P \neq 0$  and  $Q \neq 0$ .*

(ii) *The equilibrium states  $e_2^{MNPQ}$  are unstable for any nonzero reals  $M, N, P, Q$ .*

(iii) *The equilibrium states  $e_3^{MNPQ}$  are spectrally stable iff  $N = 0$ .*

(iv) *The equilibrium states  $e_4^{MNPQ}$  are spectrally stable iff  $P \neq 0$  and  $N \neq 0$ .*

(v) *The equilibrium states  $e_5^{MNP}$  are unstable for any nonzero reals  $M, N, P$ .*

(vi) *The equilibrium states  $e_6^{MN}$  are unstable for any nonzero reals  $M, N$ .*

(vii) *The equilibrium states  $e_7^{MN}$  are spectrally stable for any reals  $M, N$ .*

(viii) *The equilibrium states  $e_8^{MN}$  are unstable for any nonzero reals  $M, N$ .*

(ix) *The equilibrium states  $e_9^{MN}$  are spectrally stable iff  $M < -\frac{|N|}{\sqrt{2}}$  or  $M > \frac{|N|}{\sqrt{2}}$ .*

(x) *The equilibrium states  $e_{10}^{MNPQ}$  are spectrally stable iff  $Q \neq 0$ .*

**Proof:** Let  $A$  be the matrix of the linear part of the system (2):

$$A = \begin{pmatrix} 0 & 0 & 0 & 0 & k_3 & k_2 & 0 & 0 & 0 & 0 \\ -j_3 & 0 & -j_1 & -k_3 & 0 & -k_1 & 0 & 0 & 0 & 0 \\ j_2 & j_1 & 0 & 0 & 0 & 0 & 0 & 0 & 0 & 0 \\ 0 & 0 & -k_2 & 0 & -j_3 & 0 & h & 0 & 0 & p_1 \\ -k_3 & 0 & k_1 & j_3 & 0 & -j_1 & 0 & h & 0 & p_2 \\ 2k_2 & -k_1 & 0 & -j_2 & 2j_1 & 0 & 0 & 0 & h & p_3 \\ 0 & 0 & 0 & -h & 0 & 0 & 0 & 0 & 0 & -k_1 \\ -p_3 & 0 & 0 & 0 & -h & 0 & 0 & 0 & -j_1 & -k_2 \\ p_2 & 0 & 0 & 0 & 0 & 0 & 0 & j_1 & 0 & 0 \\ 0 & 0 & 0 & -p_1 & -p_2 & 0 & -k_1 & -k_2 & 0 & 0 \end{pmatrix}.$$

The corresponding eigenvalues of the linearized  $A(e_1)$  are  $\lambda_i = 0, i = 1, 6$ , and

$$\lambda_{7,8,9,10} = \pm \sqrt{\frac{-N^2 - P^2 - Q^2 - R^2 \pm \sqrt{-4P^2Q^2 + (N^2 + P^2 + Q^2 + R^2)^2}}{2}},$$

so the assertion follows immediately.

Similar arguments provides us all the statements.

## 4 Numerical Integration via Lie-Trotter Integrator

We shall discuss now the numerical integration of the dynamics (2) via the Lie-Trotter integrator (see [11]). For the beginning, let us observe that the Hamiltonian vector field  $X_H$  splits as follows:

$$X_H = X_{H_1} + X_{H_2} + X_{H_3} + X_{H_4},$$

where

$$H_1 = \frac{1}{2}j_1^2, \quad H_2 = \frac{1}{2}k_1^2, \quad H_3 = \frac{1}{2}k_2^2, \quad H_4 = \frac{1}{2}h^2.$$

Their corresponding integral curves are respectively given by:

$$\begin{bmatrix} j_1(t) \\ j_2(t) \\ j_3(t) \\ k_1(t) \\ k_2(t) \\ k_3(t) \\ p_1(t) \\ p_2(t) \\ p_3(t) \\ h(t) \end{bmatrix} = A_i \begin{bmatrix} j_1(0) \\ j_2(0) \\ j_3(0) \\ k_1(0) \\ k_2(0) \\ k_3(0) \\ p_1(0) \\ p_2(0) \\ p_3(0) \\ h(0) \end{bmatrix}, \quad i = 1, 2, 3, 4,$$



Then, the Lie-Trotter integrator is given by:

$$\begin{bmatrix} j_1^{n+1} \\ j_2^{n+1} \\ j_3^{n+1} \\ k_1^{n+1} \\ k_2^{n+1} \\ k_3^{n+1} \\ p_1^{n+1} \\ p_2^{n+1} \\ p_3^{n+1} \\ h^{n+1} \end{bmatrix} = A_1 A_2 A_3 A_4 \begin{bmatrix} j_1^n \\ j_2^n \\ j_3^n \\ k_1^n \\ k_2^n \\ k_3^n \\ p_1^n \\ p_2^n \\ p_3^n \\ h^n \end{bmatrix}, \quad (6)$$

i.e.

$$\left\{ \begin{array}{l} j_1^{n+1} = j_1^n + e^{dt}(-1 + e^{ct})k_3^n(t) \\ j_2^{n+1} = (-1 + e^{-bt})(-1 + e^{ct})j_1^n + j_2^n + (-1 + e^{-at})j_3^n + e^{dt}(-1 + e^{-at})(-1 + e^{-ct})k_1^n + \\ \quad + e^{dt}(-1 + e^{-at})(-1 + e^{bt})k_2^n + e^{dt}(-1 + e^{-bt})k_3^n \\ j_3^{n+1} = (-1 + e^{at})(-1 + e^{-bt})(-1 + e^{ct})j_1^n + (-1 + e^{at})j_2^n + j_3^n + e^{dt}(-1 + e^{-ct})k_1^n + \\ \quad + e^{dt}(-1 + e^{bt})k_2^n + e^{dt}(-1 + e^{at})(-1 + e^{-bt})k_3^n \\ k_1^{n+1} = (-1 + e^{ct})j_3^n + e^{dt}k_1^n \\ k_2^{n+1} = (-1 + e^{-at})(-1 + e^{ct})j_1^n + (-1 + e^{-at})(-1 + e^{-bt})j_2^n + (-1 + e^{bt})j_3^n + \\ \quad + e^{dt}(-1 + e^{bt})(-1 + e^{-ct})k_1^n + e^{dt}k_2^n + e^{dt}(-1 + e^{-at})k_3^n \\ k_3^{n+1} = (-1 + e^{ct})j_1^n + (-1 + e^{-bt})j_2^n + (-1 + e^{at})(-1 + e^{bt})j_3^n + \\ \quad + e^{dt}(-1 + e^{at})(-1 + e^{bt})(-1 + e^{-ct})k_1^n + e^{dt}(-1 + e^{at})k_2^n + e^{dt}k_3^n \\ p_1^{n+1} = e^{dt}(-1 + e^{-bt})(-1 + e^{-ct})k_2^n + p_1^n + (-1 + e^{-bt})h^n \\ p_2^{n+1} = p_2^n + (-1 + e^{-at})p_3^n + (-1 + e^{-ct})h^n \\ p_3^{n+1} = (-1 + E(at))p_2^n + p_3^n + (-1 + e^{at})(-1 + e^{-ct})h^n \\ h^{n+1} = e^{dt}(-1 + e^{-ct})k_2^n + (-1 + e^{-bt})p_1^n + h^n \end{array} \right. \quad (7)$$

Using MATHEMATICA the following can be proven:

**Theorem 4.1** *The Lie-Trotter integrator (7) has the following properties:*

- (i) *It preserves the Poisson structure  $\Pi_-$ .*
- (ii) *It preserves the Casimirs  $C_1, C_2$  of our Poisson configuration  $(iso(3, 1), \Pi_-)$ .*
- (iii) *It does not preserve the Hamiltonian  $H$  of the system (2).*

## References

- [1] S. Weinberg, *The Quantum Theory of Fields, Vol. 1: Foundations* Cambridge University Press, 1995;
- [2] M. Maggiore, *A Modern Introduction to Quantum Field Theory*, Oxford University Press, 2005;
- [3] W.-K. Tung, *Group Theory in Physics*, World Scientific, 1985;
- [4] F. Scheck, *Quantum Physics*, Springer, 2007;
- [5] B. Thaller, *The Dirac Equation*, Springer, 1992;
- [6] V. Jurdjevic, *Optimal control, geometry and mechanics*, *Mathematical control theory*, 227-267, Springer, New-York, 1999;
- [7] P. S. Krishnaprasad, *Optimal control and Poisson reduction*, *Technical Report 93-87*, Institute for System Research, University of Maryland, 1993;
- [8] A. A. Agrachev, Y. L. Sachkov, *Control theory from the geometric viewpoint*, *Encyclopedia of Mathematical Science*, 87. *Control Theory and Optimization*, II. Springer-Verlag, 2004;
- [9] R. Campoamor-Stursberg, *A new matrix method for the Casimir operators of the Lie algebras  $wsp(N, R)$  and  $Isp(2N, R)$* , *Journal of Physics A General Physics* **38(19)**: 4187, DOI 10.1088/0305-4470/38/19/009, 2005;
- [10] V. Arnold, *Conditions for nonlinear stability of stationary plane curvilinear flows of an ideal fluid*, *Doklady*, **162**, no 5, (1965) 773-777;

- [11] H. F. Trotter, On the product of semigroups of operators, *Proc. Amer. Math. Soc.* **10**, (1959) 545-551.

Camelia Pop and Ramona Ioana Iosif  
Department of Mathematics,  
Politehnica University of Timisoara,  
P-ta Victoriei 2, 300 006, Timisoara, ROMANIA  
E-mail: camelia.ariesanu@upt.ro  
E-mail: ioana\_ramo@yahoo.com

## ON THE DYNAMICS OF A HAMILTON-POISSON SYSTEM

Cristian LĂZUREANU, Camelia PETRIȘOR

### Abstract

The dynamics of a three-dimensional Hamilton-Poisson system is closely related to its constants of motion, the energy or Hamiltonian function  $H$  and a Casimir  $C$  of the corresponding Lie algebra. The orbits of the system are included in the intersection of the level sets  $H = \text{constant}$  and  $C = \text{constant}$ . Furthermore, for some three-dimensional Hamilton-Poisson systems, connections between the associated energy-Casimir mapping  $(H, C)$  and some of their dynamic properties were reported. In order to detect new connections, we construct a Hamilton-Poisson system using two smooth functions as its constants of motion. The new system has infinitely many Hamilton-Poisson realizations. We study the stability of the equilibrium points and the existence of periodic orbits. Using numerical integration we point out four pairs of heteroclinic orbits.

<sup>1</sup>

Keywords and phrases: *Hamilton-Poisson dynamics, energy-Casimir mapping, stability, periodic orbits, heteroclinic orbits, mid-point rule.*

## 1 Introduction

Many systems of first order differential equations that model processes in physics, chemistry, biology, economy, and other domains are three-dimensional systems. Some of them have two constants of motion. Consequently, they are Hamilton-Poisson systems (see, for example [18]). The dynamics of such systems takes place at the intersection of the common level sets of the Hamiltonian and the Casimir (see, for example, [8]). In [19], the energy-Casimir mapping  $\mathcal{EC} = (H, C)$  is introduced. Moreover, some connections between the dynamics of the system considered in [19] and the associated energy-Casimir mapping were given. In recent papers, the same connections and new ones were reported (see, for example, [11], [16] and therein references). These connections depend on the image of the energy-Casimir mapping. Also they depend on the partition of this image given by the images of the

---

<sup>1</sup>MSC(2010): 70H12, 70H14, 70K20, 70K42, 70K44, 65D30.

equilibrium points through  $\mathcal{EC}$ . In the most of cases the image of  $\mathcal{EC}$  is a convex set. In this paper we add a new example in the list of the systems that are analyzed by this point of view. We mention here that in our case the image of the energy-Casimir mapping is a non-convex set.

The paper is organized as follows. In Section 2, we construct a three-dimensional system of differential equations using two smooth functions as its constants of motion. One of these constants of motion is a Casimir of the Lie algebra  $\mathfrak{so}(3)$ , but the other one is a non-quadratic polynomial. We recall that quadratic Hamilton-Poisson systems on the dual space of  $\mathfrak{so}(3)$  were investigated in [1, 2]. In Section 3, using the above-mentioned Lie algebra, we give a Hamilton-Poisson realization of the considered system. Moreover, we obtain that our system has infinitely many Hamilton-Poisson realizations. In Section 4, we consider the energy-Casimir mapping  $\mathcal{EC}$  associated to the considered system. Using the images of critical points of  $\mathcal{EC}$  we give a semialgebraic partition of the image of this mapping. The connections of the energy-Casimir mapping with the dynamics of our system are pointed out in next sections. In Section 5, we prove results regarding the stability of the equilibrium points. In Section 6, we establish the topology of the fibers of the energy-Casimir mapping. We prove the existence of the periodic orbits. Using numerical simulations, we also claim the existence of heteroclinic orbits.

## 2 A construction of an integrable three-dimensional system

In this section we construct a three-dimensional system of differential equations using two smooth functions as its constants of motion.

Let  $H$  and  $C$  be two smooth functions given by

$$H(x, y, z) = \frac{1}{4}x^4 + \frac{1}{4}y^4 - \frac{1}{2}z^2, \quad C(x, y, z) = \frac{1}{2}x^2 + \frac{1}{2}y^2 + \frac{1}{2}z^2. \quad (1)$$

Consider  $x, y, z \in C^1(\mathbb{R})$  such that

$$\begin{aligned} H(x(t), y(t), z(t)) &= H(x(0), y(0), z(0)) \\ C(x(t), y(t), z(t)) &= C(x(0), y(0), z(0)), \quad \forall t \in \mathbb{R}. \end{aligned}$$

Then

$$\frac{dH}{dt} = 0, \quad \frac{dC}{dt} = 0,$$

that is

$$\begin{aligned} \frac{\partial H}{\partial x} \dot{x} + \frac{\partial H}{\partial y} \dot{y} &= -\frac{\partial H}{\partial z} \dot{z} \\ \frac{\partial C}{\partial x} \dot{x} + \frac{\partial C}{\partial y} \dot{y} &= -\frac{\partial C}{\partial z} \dot{z}. \end{aligned}$$

In our case we have

$$\begin{aligned}x^3\dot{x} + y^3\dot{y} &= z\dot{z} \\x\dot{x} + y\dot{y} &= -z\dot{z}.\end{aligned}$$

Setting

$$\dot{z} = x^3y - xy^3,$$

we get the following system

$$\begin{cases} \dot{x} = yz(1 + y^2) \\ \dot{y} = -xz(1 + x^2) \\ \dot{z} = xy(x^2 - y^2) \end{cases} \quad (2)$$

It is obvious that  $H$  and  $C$  are constants of motion of system (2). Moreover, this system is integrable and, in fact, it is a Hamilton-Poisson system.

### 3 Hamilton-Poisson realizations

In this section we give Hamilton-Poisson realizations of system (2). We obtain that the considered system is bi-Hamiltonian and in addition it has infinitely many Hamilton-Poisson realizations.

**Proposition 3.1.** *The system (2) has the Hamilton-Poisson realization*

$$(\mathfrak{so}(3)^*, \Pi_1, H),$$

where  $\mathfrak{so}(3)^*$  is the dual space of the Lie algebra  $\mathfrak{so}(3)$ , the Hamiltonian function  $H$  is given by (1) and the Poisson structure is given by

$$\Pi_1 = \begin{bmatrix} 0 & z & -y \\ -z & 0 & x \\ y & -x & 0 \end{bmatrix}. \quad (3)$$

*Proof.* It is known that the function  $C$  given by (1) is a Casimir of the Lie algebra  $\mathfrak{so}(3)$  (see, e.g. [1]), where

$$\mathfrak{so}(3) = \left\{ X = \begin{bmatrix} 0 & -w & v \\ w & 0 & -u \\ -v & u & 0 \end{bmatrix} : u, v, w \in \mathbb{R} \right\}.$$

We immediately obtain  $\Pi_1 \cdot \nabla C = \mathbf{0}$  and  $\Pi_1 \cdot \nabla H = \dot{\mathbf{x}}^t$ ,  $\mathbf{x} = (x, y, z)$ .  $\square$

**Proposition 3.2.** *The system (2) is a bi-Hamiltonian system.*

*Proof.* Considering the second Poisson structure

$$\Pi_2 = \begin{bmatrix} 0 & z & y^3 \\ -z & 0 & -x^3 \\ -y^3 & x^3 & 0 \end{bmatrix}, \quad (4)$$

it follows that system (2) has the Hamilton-Poisson realization  $(\mathbb{R}^3, \Pi_2, C)$ , where  $C$  is given by (1). Furthermore the function  $H$  (1) fulfills  $\Pi_2 \cdot \nabla H = \mathbf{0}$ .

Because  $\Pi_1 \cdot \nabla H = \Pi_2 \cdot \nabla C = \dot{\mathbf{x}}^t$  and  $\Pi_1$  and  $\Pi_2$  are compatible Poisson structures, the conclusion follows.  $\square$

Using the above results, we obtain the Poisson structure  $\Pi_{a,b} = a\Pi_1 - b\Pi_2$ ,  $a, b \in \mathbb{R}$ . Consider  $c, d \in \mathbb{R}$  such that  $ad - bc = 1$  and  $H_{c,d} = cC + dH$ ,  $C_{a,b} = aC + bH$ . We have  $\Pi_{a,b} \cdot \nabla H_{c,d} = \dot{\mathbf{x}}^t$  and  $\Pi_{a,b} \cdot \nabla C_{a,b} = \mathbf{0}$ . Therefore we have proven the next result.

**Proposition 3.3.** *There exist infinitely many Hamilton-Poisson realizations of system (2), namely  $(\mathbb{R}^3, \Pi_{a,b}, H_{c,d})$ , where*

$$\Pi_{a,b} = \begin{bmatrix} 0 & (a-b)z & -ay + by^3 \\ (b-a)z & 0 & ax - bx^3 \\ ay - by^3 & -ax + bx^3 & 0 \end{bmatrix},$$

and

$$H_{c,d}(x, y, z) = \frac{d}{4}(x^4 + y^4) + \frac{c}{2}(x^2 + y^2) + \frac{c-d}{2}z^2,$$

for every  $a, b, c, d \in \mathbb{R}$  such that  $ad - bc = 1$ .

## 4 Energy-Casimir mapping

In the geometric frame given by Proposition 3.1, in this section we study some properties of the energy-Casimir mapping  $\mathcal{EC}$  associated to system (2). We present the image of this mapping. In addition, using the critical points of  $\mathcal{EC}$  we obtain a partition of the image of the energy-Casimir mapping. This partition gives some connections with the dynamics of the considered system.

Consider the Hamiltonian  $H$  and a Casimir function  $C$  given by (1). The energy-Casimir mapping is given below

$$\mathcal{EC} : \mathbb{R}^3 \rightarrow \mathbb{R}^2, \quad \mathcal{EC}(x, y, z) = \left( \frac{1}{4}x^4 + \frac{1}{4}y^4 - \frac{1}{2}z^2, \frac{1}{2}x^2 + \frac{1}{2}y^2 + \frac{1}{2}z^2 \right). \quad (5)$$

The image of the energy-Casimir mapping is the set

$$\text{Im}(\mathcal{EC}) = \{(h, c) \in \mathbb{R}^2 \mid (\exists)(x, y, z) \in \mathbb{R}^3 : \mathcal{EC}(x, y, z) = (h, c)\}.$$

**Proposition 4.1.** *Let  $\mathcal{EC}$  be the energy-Casimir mapping (5) associated to system (2). Then*

$$\text{Im}(\mathcal{EC}) = \{(h, c) \in \mathbb{R}^2 \mid c \geq -h, c \geq \sqrt{h}\}. \quad (6)$$

*Proof.* The pair  $(h, c)$  belongs to  $\text{Im}(\mathcal{EC})$  if and only if the system

$$\frac{1}{4}x^4 + \frac{1}{4}y^4 - \frac{1}{2}z^2 = h, \quad \frac{1}{2}x^2 + \frac{1}{2}y^2 + \frac{1}{2}z^2 = c$$

is compatible. Performing algebraic computations, we get the conclusion.  $\square$

**Remark 4.2.** *The energy-Casimir mappings of some particular Hamilton-Poisson systems were studied in many papers. In some cases the image of  $\mathcal{EC}$  is  $\mathbb{R}^2$  [6, 20], in other cases it is a closed convex subset of  $\mathbb{R}^2$  [7, 9, 10, 11, 12, 13, 14, 15, 19]. In [16]  $\text{Im}(\mathcal{EC})$  is not a closed set. In our case the image of the considered energy-Casimir mapping is shown in Figure 1. It is a closed non-convex set, what explains while we choose those constants of motion given by (1).*

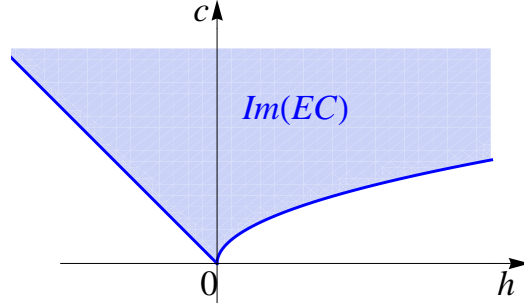


Figure 1: The image of the energy-Casimir mapping.

A point  $(x_0, y_0, z_0) \in \mathbb{R}^3$  is a critical point of the energy-Casimir mapping if the rank of the Jacobian matrix of  $\mathcal{EC}$  at this point is less than 2.

**Proposition 4.3.** *The critical points of the energy-Casimir mapping (5) are given by the following families*

$$E_1(M, 0, 0), E_2(0, M, 0), E_3(0, 0, M), E_4(M, M, 0), E_5(M, -M, 0), M \in \mathbb{R}. \quad (7)$$

*Proof.* We have

$$D\mathcal{EC}(x, y, z) = \begin{bmatrix} DH(x, y, z) \\ DC(x, y, z) \end{bmatrix} = \begin{bmatrix} x^3 & y^3 & -z \\ x & y & z \end{bmatrix}.$$

Imposing the condition  $\text{rank } D\mathcal{EC} < 2$ , the conclusion follows.  $\square$

Now we determine the images of these critical points through the energy-Casimir mapping. We have

$$\begin{aligned}\mathcal{E}\mathcal{C}(E_1) &= \mathcal{E}\mathcal{C}(E_2) = \left(\frac{1}{4}M^4, \frac{1}{2}M^2\right) = (h, c), \quad c = \sqrt{h}, \quad h \geq 0, \\ \mathcal{E}\mathcal{C}(E_3) &= \left(-\frac{1}{2}M^2, \frac{1}{2}M^2\right) = (h, c), \quad c = -h, \quad h \leq 0, \\ \mathcal{E}\mathcal{C}(E_4) &= \mathcal{E}\mathcal{C}(E_5) = \left(\frac{1}{2}M^4, M^2\right) = (h, c), \quad c = \sqrt{2h}, \quad h \geq 0.\end{aligned}$$

The images through the energy-Casimir mapping of its critical points are given by the curves (see Figure 2)

$$\begin{aligned}\Sigma_{1,2}^s &= \{(h, c) : c = \sqrt{h}, \quad h \geq 0\}, \\ \Sigma_3^s &= \{(h, c) : c = -h, \quad h \leq 0\}, \\ \Sigma_{4,5}^u &= \{(h, c) : c = \sqrt{2h}, \quad h > 0\}.\end{aligned}$$

We also consider the sets

$$\begin{aligned}\Sigma_p^1 &= \{(h, c) : \sqrt{h} < c < \sqrt{2h}, \quad h > 0\}, \\ \Sigma_p^2 &= \{(h, c) : c > -h, \quad h < 0\} \cup \{(h, c) : c > \sqrt{2h}, \quad h > 0\}.\end{aligned}$$

**Remark 4.4.** *The images of the critical points through the energy-Casimir mapping lead to the following partition of the image of the energy-Casimir mapping*

$$\text{Im}(\mathcal{E}\mathcal{C}) = \Sigma_{1,2}^s \cup \Sigma_p^1 \cup \Sigma_{4,5}^u \cup \Sigma_p^2 \cup \Sigma_3^s. \quad (8)$$

*Note that there is only one bifurcation point in this partition, namely  $(0, 0)$ .*

As it has been reported in the above-mentioned papers (Remark 4.2), there are some connections between the partition of the image of the energy-Casimir mapping and the dynamics of the corresponding system. More precisely, in the case when  $\text{Im}(\mathcal{E}\mathcal{C})$  is a proper convex subset of  $\mathbb{R}^2$  its boundary is the union of the images of the nonlinearly stable equilibrium points through  $\mathcal{E}\mathcal{C}$ . Moreover, if a curve that gives the partition and belongs to the interior of  $\text{Im}(\mathcal{E}\mathcal{C})$  do not have bifurcation points, then it is given by the images of the unstable equilibrium points through  $\mathcal{E}\mathcal{C}$ . Furthermore, if such a curve is an arc of parabola, then homoclinic orbits were computed. In addition, the open subsets  $\Sigma_p$  of  $\text{Im}(\mathcal{E}\mathcal{C})$  are related to periodic orbits.

In our case  $\text{Im}(\mathcal{E}\mathcal{C})$  is a non-convex set. Therefore it is natural to ask whether these properties remain true, namely the critical points  $E_1, E_2, E_3$  are stable equilibrium points and  $E_4, E_5$  are unstable, and also there are periodic orbits in the considered dynamics. Moreover, are there homoclinic orbits?

In next sections we give answers to these questions.

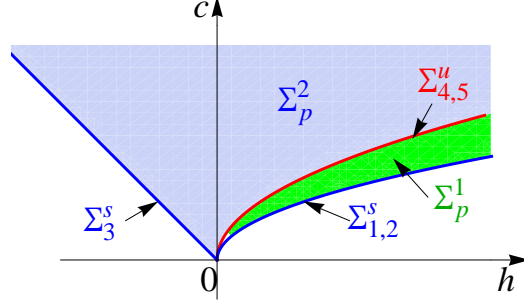


Figure 2: The semialgebraic partition of the image of the energy-Casimir mapping given by the critical points.

## 5 Stability

In this section we study the stability of the equilibrium points of system (2). We use Arnold stability test [3], Lyapunov functions, and First Lyapunov's Stability Criterion [17].

It is easy to see that system (2) takes the form  $\dot{\mathbf{x}} = \nabla H \times \nabla C$ ,  $\mathbf{x} = (x, y, z)$ . Therefore the equilibrium points of system (2) are in fact the critical points (7) of the energy-Casimir mapping (5).

In the next proposition we give the results regarding the stability of the equilibrium points

$$E_1(M, 0, 0), E_2(0, M, 0), E_3(0, 0, M), E_4(M, M, 0), E_5(M, -M, 0), M \in \mathbb{R}.$$

**Proposition 5.1.** *a) The points  $E_1, E_2, E_3$  are nonlinearly stable equilibrium points for every  $M \in \mathbb{R}$ .*

*b) The equilibrium points  $E_4, E_5$  are unstable for every  $M \in \mathbb{R}, M \neq 0$ .*

*Proof.* a) Let  $M \in \mathbb{R}, M \neq 0$  and the equilibrium point  $E_1(M, 0, 0)$ . We consider the function  $F = H + \lambda C$ . The condition  $\nabla F(M, 0, 0) = \mathbf{0}$  leads to  $\lambda = -M^2$ . Using the fact that  $dC(M, 0, 0) = 0$ , we obtain  $d^2F(M, 0, 0) = -M^2 dy^2 - (M^2 + 1) dz^2$  that is negative definite. By Arnold stability test we deduce that the equilibrium point  $E_1$  is nonlinearly stable. We analogously proceed for the equilibrium points  $E_2$  and  $E_3$ .

If  $M = 0$ , then all the equilibrium points coincide. In this case the Casimir  $C(x, y, z) = \frac{1}{2}x^2 + \frac{1}{2}y^2 + \frac{1}{2}z^2$  is a Lyapunov function for the equilibrium point  $(0, 0, 0)$  and  $\frac{dC}{dt} = 0$ . Therefore the equilibrium point  $(0, 0, 0)$  is nonlinearly stable.

b) Let  $J(x, y, z)$  be the matrix of linear part of system (2), that is

$$J(x, y, z) = \begin{bmatrix} 0 & 3y^2z + z & y^3 + y \\ -3x^2z - z & 0 & -x^3 - x \\ 3x^2y - y^3 & x^3 - 3xy^2 & 0 \end{bmatrix}.$$

The characteristic roots of  $J(E_4)$  and  $J(E_5)$  are given by

$$\lambda_1 = 0, \quad \lambda_{2,3} = \pm 2M^2 \sqrt{M^2 + 1}.$$

Therefore, for every  $M \in \mathbb{R}$ ,  $M \neq 0$  there is a positive eigenvalue and consequently the equilibrium points  $E_4$  and  $E_5$  are unstable.  $\square$

**Remark 5.2.** *The images of the nonlinearly stable equilibrium points through the energy-Casimir mapping are the curves  $\Sigma_{1,2}^s$  and  $\Sigma_3^s$ , where the superscript “s” means stable, as in above-mentioned papers. Moreover, the set  $\Sigma_{4,5}^u$  is the image of the unstable equilibrium points through  $\mathcal{EC}$ .*

## 6 Fibers of the energy-Casimir mapping

The fiber of the energy-Casimir mapping  $\mathcal{EC}$  corresponding to an element  $(h_0, c_0) \in \text{Im}(\mathcal{EC})$  is the set

$$\mathcal{F}_{(h_0, c_0)} = \{(x, y, z) \in \mathbb{R}^3 \mid \mathcal{EC}(x, y, z) = (h_0, c_0)\}. \quad (9)$$

The implicit equation of the above fiber is given by

$$\mathcal{F}_{(h_0, c_0)} : \begin{cases} H(x, y, z) = h_0 \\ C(x, y, z) = c_0 \end{cases}. \quad (10)$$

On the other hand the dynamics of the considered system takes place at the intersection of the level sets  $H(x, y, z) = \text{constant}$ ,  $C(x, y, z) = \text{constant}$ . Therefore an orbit of the our system is given implicitly by the above fiber.

Taking into account the partition (8) of  $\text{Im}(\mathcal{EC})$ , in this section we point out the topology of the fibers of energy-Casimir mapping (5). We prove the existence of the periodic orbits. Using numerical integration, we emphasize a possible existence of some heteroclinic cycles.

Let  $M > 0$ . Fixing  $c = c_0 > 0$  and varying  $h$  such that  $-c_0 \leq h \leq c_0^2$ , the straight-line of equation  $c = c_0$  intersects all the sets of the partition (8) of the image of the energy-Casimir mapping. The intersections of the level sets  $H(x, y, z) = h$  and  $C(x, y, z) = c_0$  when  $(h, c_0)$  belongs to  $\Sigma_{1,2}^s$ ,  $\Sigma_p^1$ ,  $\Sigma_{4,5}^u$ ,  $\Sigma_p^2$ , and  $\Sigma_3^s$  are presented in Figure 3 (a), (b), (c), (d)-(e), and (f) respectively. We notice that around the

equilibrium points  $E_1(\pm M, 0, 0)$  and  $E_2(0, \pm M, 0)$  (Figure 3 (a)) there are four families of periodic orbits (Figure 3 (b)) which collide (Figure 3 (c)) when  $h$  decreases and takes the value  $\frac{1}{2}c_0^2$ . Four orbits are obtained and they are contained in the intersection of the level sets  $H(x, y, z) = h$  and  $C(x, y, z) = c_0$ , where  $(h, c_0) \in \Sigma_{4,5}^u$ . Also, in this case, the fiber  $\mathcal{F}_{(h,c)}$  contains the unstable equilibrium points  $E_4$  and  $E_5$ . Afterwards these orbits split in two families of periodic orbits around  $E_3(0, 0, \pm M)$  (Figure 3 (d),(e)) which tend to  $E_3$  as  $h \rightarrow -c_0$  (Figure 3 (f)). Therefore we deduce that apparently the above-mentioned four orbits are heteroclinic orbits.

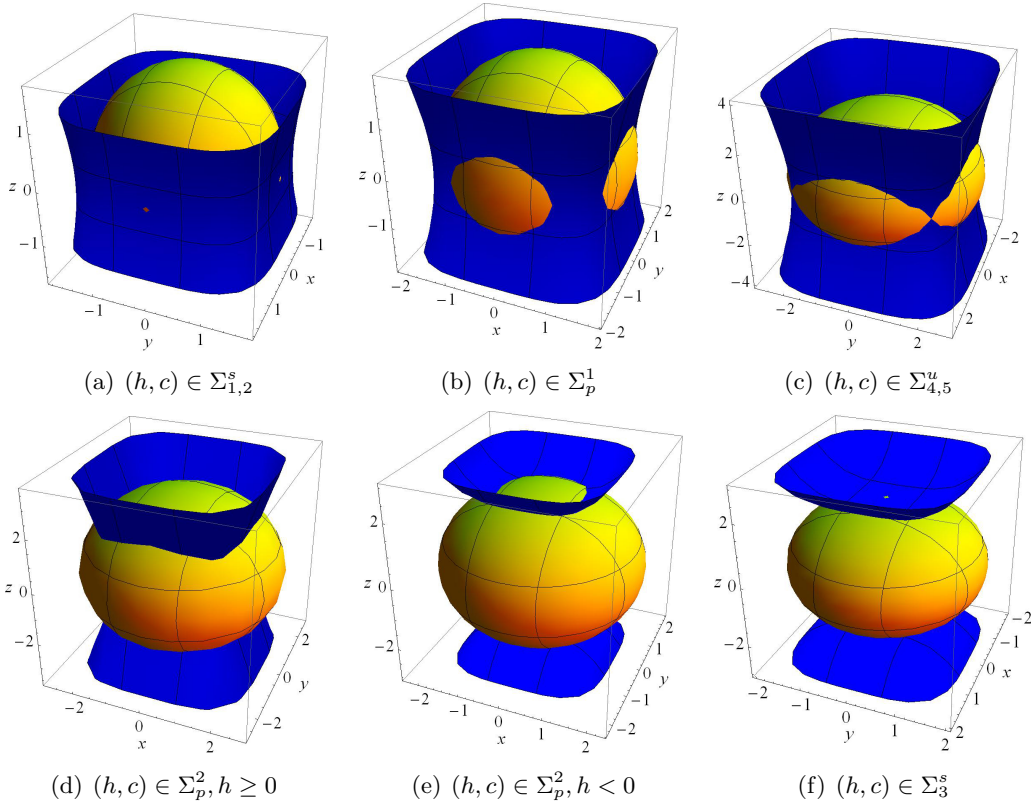


Figure 3: Intersections of the level sets  $H(x, y, z) = h$  and  $C(x, y, z) = c$ , namely (a) and (f): stable equilibrium points; (b),(d),(e): periodic orbits; (c): heteroclinic orbits.

We begin our study with the pairs  $(h, c)$  that belong to the boundary of  $\text{Im}(\mathcal{E}\mathcal{C})$ .

**Proposition 6.1.** *Let  $(h, c) \in \Sigma_{1,2}^s \cup \Sigma_3^s$ . Then the corresponding fiber contains only nonlinear stable equilibrium points, namely:*

a) *If  $(h, c) \in \Sigma_{1,2}^s$ , then  $\mathcal{F}_{(h,c)} = \{(\pm\sqrt{2c}, 0, 0)\} \cup \{(0, \pm\sqrt{2c}, 0)\}$  (Figure 3 (a));*

- b) If  $(h, c) \in \Sigma_3^s$ , then  $\mathcal{F}_{(h,c)} = \{(0, 0, \pm\sqrt{2c})\}$  (Figure 3 (f));  
 c) If  $(h, c) \in \Sigma_{1,2}^s \cap \Sigma_3^s$ , then  $\mathcal{F}_{(h,c)} = \{(0, 0, 0)\}$ .

*Proof.* a) By hypothesis,  $c = \sqrt{h}$ . Using (9) and (1), we obtain

$$z^2(z^2 + 2 + 2x^2 + 2y^2) + 2x^2y^2 = 0.$$

Hence  $z = 0$  and  $xy = 0$ . Therefore the conclusion follows.

Analogously we prove b) and c). □

We study the others cases in the next subsections.

## 6.1 Periodic orbits

Let  $(h, c) \in \Sigma_p^1 \cup \Sigma_p^2$ , where  $\Sigma_p^1$  and  $\Sigma_p^2$  are given by (8). The intersection of the level sets  $H(x, y, z) = h$  and  $C(x, y, z) = c$  suggests the existence of the periodic orbits (see Figure 3 (b),(d),(e)). We prove the existence of these periodic orbits around the nonlinear stable equilibrium points using a version of Moser's theorem in the case of zero eigenvalue [5].

**Proposition 6.2.** *Let  $E_1 = (M, 0, 0)$  be a nonlinear stable equilibrium point of system (2) such that  $M \in \mathbb{R}^*$ . Then for each sufficiently small  $\varepsilon \in \mathbb{R}_+^*$ , any integral surface*

$$\Sigma_\varepsilon^{E_1} : -\frac{1}{4}(x^4 + y^4) + \frac{M^2}{2}(x^2 + y^2) + \frac{M^2 + 1}{2}z^2 - \frac{1}{4}M^4 = \varepsilon^2$$

*contains at least one periodic orbit  $\gamma_\varepsilon^{E_1}$  of system (2) whose period is close to  $\frac{2\pi}{M^2\sqrt{M^2+1}}$ .*

*Proof.* We apply Theorem 2.1 from [5].

The characteristic polynomial associated with the linearization of system (2) at  $E_1$  has the eigenvalues  $\lambda_1 = 0$  and  $\lambda_{2,3} = \pm iM^2\sqrt{M^2+1}$ . Furthermore, the eigenspace corresponding to the eigenvalue zero is  $\text{span}_{\mathbb{R}}\{(1, 0, 0)\}$ . The constant of motion of system (2) given by

$$I(x, y, z) = -\frac{1}{4}(x^4 + y^4) + \frac{M^2}{2}(x^2 + y^2 + z^2)$$

has the properties:  $dI(M, 0, 0) = 0$  and  $d^2I(M, 0, 0)|_{W \times W} = M^2dy^2 + (M^2+1)dz^2 > 0$ , where  $W = \ker dC(M, 0, 0) = \text{span}_{\mathbb{R}}\{(0, 1, 0), (0, 0, 1)\}$ .

Therefore the conclusion follows via Theorem 2.1 [5]. □

We obtain the same result for  $E_2$ . Analogously we get the next result.

**Proposition 6.3.** *Let  $E_3 = (0, 0, M)$  be a nonlinear stable equilibrium point of system (2) such that  $M \in \mathbb{R}^*$ . Then for each sufficiently small  $\varepsilon \in \mathbb{R}_+^*$ , any integral surface*

$$\Sigma_\varepsilon^{E_1} : \frac{1}{4}(x^4 + y^4) + \frac{1}{2}(x^2 + y^2) = \varepsilon^2$$

*contains at least one periodic orbit  $\gamma_\varepsilon^{E_3}$  of system (2) whose period is close to  $\frac{2\pi}{|M|}$ .*

## 6.2 Numerical integration. Heteroclinic orbits

Consider  $(h, c) \in \Sigma_{4,5}^u$ , that is  $h > 0$  and  $c = \sqrt{2h}$ . The fiber  $\mathcal{F}_{(h,c)}$  contains the unstable equilibrium points  $E_4$  and  $E_5$ . Its implicit equation is given by

$$\frac{1}{4}x^4 + \frac{1}{4}y^4 - \frac{1}{2}z^2 = \frac{c^2}{2}, \quad \frac{1}{2}x^2 + \frac{1}{2}y^2 + \frac{1}{2}z^2 = c. \quad (11)$$

The intersection of the above level sets is shown in Figure 3 (c) and it suggests the existence of four pair of heteroclinic orbits that connect the unstable equilibrium points  $E_4(\pm\sqrt{c}, \pm\sqrt{c}, 0)$  and  $E_5(\pm\sqrt{c}, \mp\sqrt{c}, 0)$ .

We recall that a heteroclinic orbit  $\mathcal{HE} : \mathbb{R} \rightarrow \mathbb{R}^3$  is a solution  $(x(t), y(t), z(t))$  of the considered system that connects two unstable equilibrium points  $e_1$  and  $e_2$  of the system, that is  $\mathcal{HE}(t) := (x(t), y(t), z(t))$  and  $\mathcal{HE}(t) \rightarrow e_1$  as  $t \rightarrow -\infty$ ,  $\mathcal{HE}(t) \rightarrow e_2$  as  $t \rightarrow \infty$ .

We give the numerical simulation of these heteroclinic orbits applying the mid-point rule (see [4] and references therein) to system (2).

Consider the Hamilton-Poisson realization of system (2) given by Proposition 3.1:

$$\dot{\mathbf{x}} = \Pi_1(\mathbf{x})\nabla H(\mathbf{x}), \quad \mathbf{x} = (x, y, z)^t,$$

where  $\Pi_1$  is the Poisson structure (3) and  $H$  is the Hamiltonian function. The mid-point rule is given by the following implicit recursion [4]

$$\frac{\mathbf{x}_{k+1} - \mathbf{x}_k}{\Delta t} = \Pi_1\left(\frac{\mathbf{x}_k + \mathbf{x}_{k+1}}{2}\right)\nabla H\left(\frac{\mathbf{x}_k + \mathbf{x}_{k+1}}{2}\right),$$

where  $\Delta t$  is the time-step. “If  $\Pi(\mathbf{x})$  is linear in  $\mathbf{x}$ , then the mid-point rule is an almost Poisson integrator, that is it preserve the Poisson structure up to second order” [4]. Furthermore, “the mid-point rule preserves exactly any conserved quantity having only linear and quadratic terms” [4].

The integrator for system (2) is given by

$$\begin{aligned} \frac{x_{k+1} - x_k}{\Delta t} &= \frac{1}{16}(y_k + y_{k+1})(z_k + z_{k+1})(4 + (y_k + y_{k+1})^2) \\ \frac{y_{k+1} - y_k}{\Delta t} &= -\frac{1}{16}(x_k + x_{k+1})(z_k + z_{k+1})(4 + (x_k + x_{k+1})^2) \\ \frac{z_{k+1} - z_k}{\Delta t} &= \frac{1}{16}(x_k + x_{k+1})(y_k + y_{k+1})((x_k + x_{k+1})^2 - (y_k + y_{k+1})^2) \end{aligned} \quad (12)$$

**Remark 6.4.** *Because the Poisson bracket (3) is linear, the mid-point rule of system (2) given by (12) is an almost Poisson integrator. Moreover, the Casimir  $C$  (1) is quadratic, hence it is preserved by this integrator.*

We implemented algorithm (12) in Wolfram Mathematica<sup>TM</sup>.

First, we fix  $h = 0.5$ ,  $c = \sqrt{2h} = 1$ , and  $z_1 = 0.5$  and compute  $x_1, y_1$  such that  $H(x_1, y_1, z_1) = h$  and  $C(x_1, y_1, z_1) = c$ . We find eight solutions and we take  $x_1 = 1.25338$  and  $y_1 = 0.42312$ . Choosing the time-step  $\Delta t = 0.015$ , after 160 iterations we get the point  $(1.00305, -0.996944, 0.00128394)$  which is closer to the unstable equilibrium point  $E_5(1, -1, 0)$ . To simulate the behavior of the orbit when  $t$  decreases to  $-\infty$ , we consider the same initial point  $(x_1, y_1, z_1)$  and  $\Delta t = -0.015$ . After 160 iterations we get the point  $(1.00438, 0.995591, -0.00465251)$  which is closer to the unstable equilibrium point  $E_4(1, 1, 0)$ . The discrete orbit is shown in Figure 4 (a). We remark that the points  $(x_k, y_k, z_k)$  are very close near the both unstable equilibrium points. Analogously we obtain a second orbit that connects the points  $E_4(1, 1, 0)$  and  $E_5(1, -1, 0)$  (Figure 4 (b)).

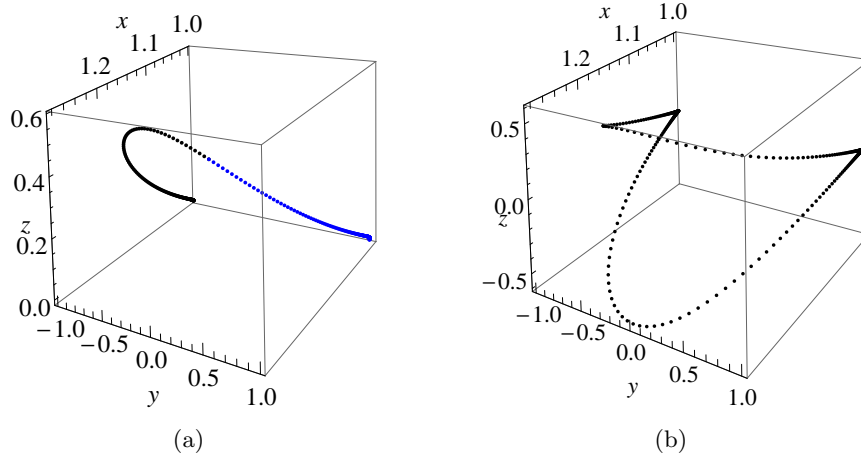


Figure 4: Numerical simulation of heteroclinic orbits: (a) an orbit; (b) a pair of orbits.

In Figure 5 the obtained pair of orbits is shown together with the intersection of the level sets  $H(x, y, z) = \frac{1}{2}$  and  $C(x, y, z) = 1$  which correspond to the equilibrium points  $E_4(1, 1, 0)$ ,  $E_5(1, -1, 0)$ . We notice a very well superposition of these curves.

In the same manner we obtain the others “heteroclinic” orbits (Figure 6 (a)). They arise naturally taking into account the symmetries of system (2) given by the transformations  $(x, y, z) \rightarrow (-x, -y, z)$ ,  $(x, y, z) \rightarrow (-x, y, -z)$ ,  $(x, y, z) \rightarrow (x, -y, -z)$ ,  $(x, y, z) \rightarrow (-y, x, z)$ ,  $(x, y, z) \rightarrow (y, -x, z)$ . We also remark that the

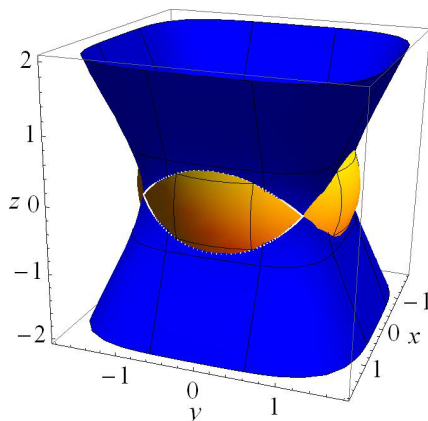


Figure 5: A pair of heteroclinic orbits and the intersection of the level sets  $H = c^2/2$ ,  $C = c$ .

unstable equilibrium points  $E_4(1, 1, 0)$ ,  $E_5(-1, 1, 0)$ ,  $E_4(-1, -1, 0)$ , and  $E_5(1, -1, 0)$  are connected by two cycles of “heteroclinic” orbits. Such a cycle is shown in Figure 6 (b).

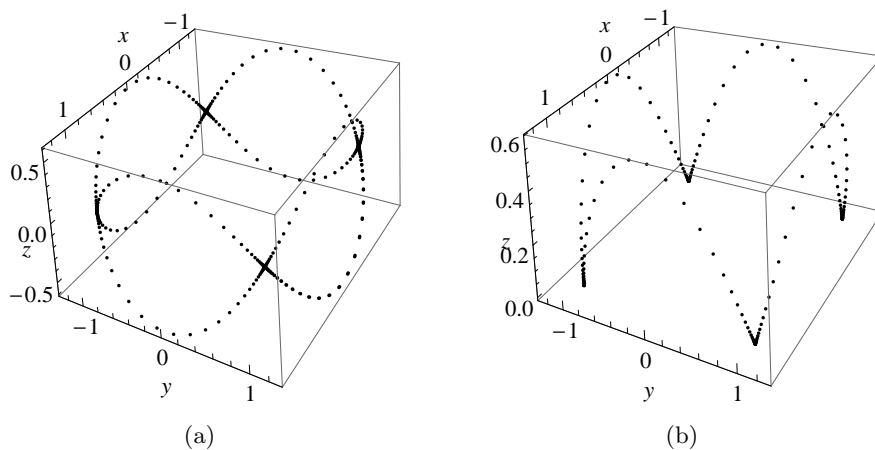


Figure 6: Numerical simulation of heteroclinic orbits: (a) four pairs of orbits; (b) a cycle of orbits.

## 7 Acknowledgments

This work was supported by research grants PCD-TC-2017.

## References

- [1] R. M. Adams, R. Biggs, C. C. Remsing, Quadratic Hamiltonian-Poisson systems on  $so(3)_*$ : classification and integration, in *Geometry, integrability and quantization XV*, Avangard Prima, Sofia, (2014), 55–66.
- [2] R. M. Adams, R. Biggs, W. Holderbaum, C. C. Remsing, On the stability and integration of Hamilton-Poisson systems on  $so(3)_*$ , *Rendiconti di Matematica*, Serie VII, **37**, (2016), 1–42.
- [3] V. Arnold, Conditions for nonlinear stability of stationary plane curvilinear flows on an ideal fluid, *Doklady Akademii Nauk SSSR*, **162**(5), (1965), 773–777.
- [4] M. A. Austin, P. S. Krishnaprasad, Li-Sheng Wang, Almost Poisson Integration of Rigid Body Systems, *Journal of Computational Physics*, **107**(1), (1993), 105–117.
- [5] P. Birtea, M. Puta, R. M. Tudoran, Periodic orbits in the case of zero eigenvalue, *C.R. Acad. Sci. Paris*, Ser. I, **344**, (2007), 779–784.
- [6] T. Bînzar, C. Lăzureanu, On some dynamical and geometrical properties of the Maxwell-Bloch equations with a quadratic control, *Journal of Geometry and Physics*, **70**, (2013), 1–8.
- [7] T. Bînzar, C. Lăzureanu, A Rikitake type system with one control, *Discrete and Continuous Dynamical Systems-B* **18**(7), (2013), 1755–1776.
- [8] D. D. Holm, J. E. Marsden, The rotor and the pendulum, in *Symplectic Geometry and Mathematical Physics*, Prog. Math. 99, P. Donato, C. Duval, J. Elhadad, and G. M. Tuynman, eds., Birkhäuser, Boston, Cambridge, MA, (1991), 189–203.
- [9] C. Lăzureanu, On the Hamilton-Poisson realizations of the integrable deformations of the Maxwell-Bloch equations, *Comptes Rendus Mathématique*, **355**(5), (2017), 596–600.
- [10] C. Lăzureanu, Hamilton-Poisson Realizations of the Integrable Deformations of the Rikitake System, *Advances in Mathematical Physics*, **2017**, (2017), Article ID 4596951, 9 pages.
- [11] C. Lăzureanu, On a Hamilton–Poisson approach of the Maxwell–Bloch equations with a control, *Mathematical Physics, Analysis and Geometry*, (2017), 20: 20.
- [12] C. Lăzureanu, The real-valued Maxwell–Bloch equations with controls: From a Hamilton–Poisson system to a chaotic one, *International Journal of Bifurcation and Chaos*, **27**, (2017), 1750143-1–17.

- [13] C. Lăzureanu, T. Bînzar, A Rikitake type system with quadratic control, *International Journal of Bifurcation and Chaos*, **22**(11), (2012), 1250274, 14 pages.
- [14] C. Lăzureanu, T. Bînzar, Some geometrical properties of the Maxwell-Bloch equations with a linear control, *Proc. of the XIII-th Int. Conf. Math. App.*, Timișoara, 2012, 151–158.
- [15] C. Lăzureanu, T. Bînzar, Symmetries and properties of the energy-Casimir mapping in the ball-plate problem, *Advances in Mathematical Physics*, **2017**, (2017), Article ID 5164602, 13 pages.
- [16] C. Lăzureanu, C. Petrișor, Stability and Energy-Casimir Mapping for Integrable Deformations of the Kermack-McKendrick System, *Advances in Mathematical Physics*, **2018**, (2018), Article ID 5398768, 9 pages.
- [17] A. M. Lyapunov, Problème générale de la stabilité du mouvement, vol. 17, Princeton University Press, Princeton, NJ, USA, 1949.
- [18] R. M. Tudoran, A normal form of completely integrable systems, *Journal of Geometry and Physics*, **62**(5), (2012), 1167–1174.
- [19] R. M. Tudoran, A. Aron, Ș. Nicoară, On a Hamiltonian Version of the Rikitake System, *SIAM Journal on Applied Dynamical Systems*, **8**(1), (2009), 454–479.
- [20] R. M. Tudoran, A. Gîrban, On a Hamiltonian version of a three-dimensional Lotka-Volterra system, *Nonlinear Analysis: Real World Applications*, **13**, (2012), 2304–2312.

Cristian Lăzureanu and Camelia Petrișor  
Department of Mathematics,  
Politehnica University of Timisoara,  
P-ta Victoriei 2, 300 006, Timisoara, ROMANIA  
E-mail: cristian.lazureanu@upt.ro  
E-mail: camelia.petrisor@upt.ro

## SOME PROPERTIES OF CORTICAL BONES

Ioana Ramona IOSIF

### Abstract

In this paper are presented: structure of the bone tissue, anisotropic linear-elastic models of cortical bone and Analysis numerical propagation of a cracks into the cortical bone. To determine the fracture mechanics parameters at the crack tip, the finite element method was implemented in the FRANC2D / L 1.5 software. <sup>1</sup>

Keywords and phrases: *cortical bone, anisotropic, FRANC2D / L*

## 1 The structure of the bone tissue

The tissue has a complex hierarchical structure (Figure 1) which, due to its reduced density, results in a unique combination of properties: high strength and toughness, good stiffness, absorption capacity of deformation energy, Taylor (2010).

Also, this complex structure allows the bone tissue to perform important mechanical, biological and chemical functions, Sabet(2018):

- The structural support, ensuring body shape and weight support;
- It forms cavities for the protection of internal organs (the cranial box, thorax box, vertebral canal, etc.);
- Mineral ion homeostasis, bone tissue depositing 99% of the total  $Ca^{2+}$  in the body, 85% of the total phosphorus and 66% of the total magnesium);
- The spongy tissue of the epiphyses hosts the hematopoietic tissue (red marrow);
- The regenerative function that provides bone remodeling, healing of cracks and fractures. Bone tissue is divided into two broad categories, namely, compact bone tissue (osul cortical) and spongy bone (trabecular bone), see Figure 1. The compact bone tissue, accounting for 80% of the bone mass, represents a dense structure that contributes to strength and rigidity of the bone. It is located in the diaphysis of the long bones and in the cortical bones. Spongy bone tissue forms a less dense structure and is located in the central area of short bones, epiphyses of long bones

---

<sup>1</sup>MSC (2010): 74R99

and diploid bones. It is responsible for the absorption of deformation energy and the distribution of forces in the body. At the nanometric scale, collagen molecules and apatite crystals constitute collagen mineralized with a diameter of about 100 nm and a length of several  $\mu\text{m}$ , Sabet (2016), see Figure 1.

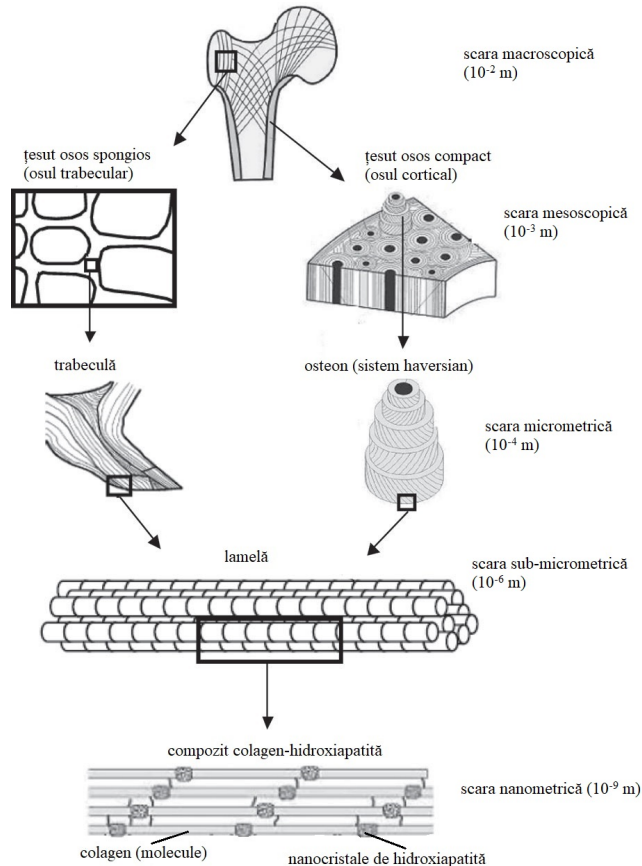


Figure 1:

These mineralized fibers, placed parallel to each other, form sub-micrometric scaffolds with a thickness of 3-7  $\mu\text{m}$ , called lamellas. On a micrometric scale, the assembling of the lamellae leads to the formation of a number of tissues, the compact bone and the spongios. Compact (cortical) structure, approximately 4-20 lamellae, not concentrically disposed around a vascular channel (haversian canal) forming the osteon, 200-300  $\mu\text{m}$  in diameter a few mm. Between the osteons is the interstitial tissue, formed by remnants of the aged osteoarthritis, resulting from the bone remodeling process. Separation is provided by a cement line containing less collagen

(mesoscopic scale, see Figure 2).

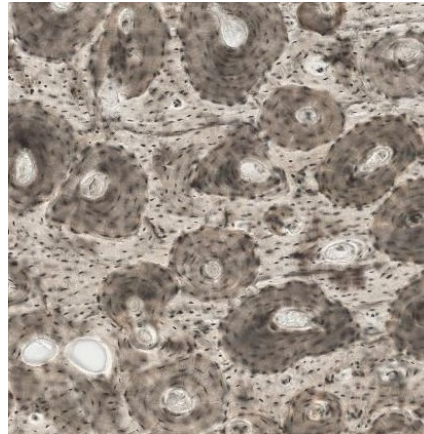


Figure 2:

In the structure of the spongy trabecular bone, the lamellele are assembled into branched trabecular forming a network that delimits areolele of different shapes and sizes. Areas contain connective tissue, blood vessels, nerve endings, and bone marrow. Thus, on a mesoscopic scale results a cellular structure illustrated in Figure 3. On a macroscopic scale the bone contains both compact tissue and spongy tissue.

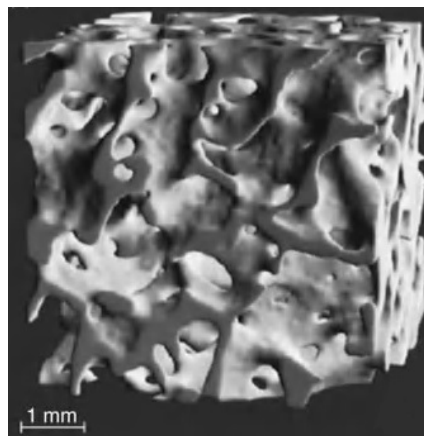


Figure 3:

The composition of the human bone depends on a large number of factors: sex, age, type of tissue, site of sampling, Katz (2008). Thus, bone tissue is thought

to contain 32 – 44% organic substance (mainly collagen), 33 – 43% minerals (as hydroxyapatite) and 15 – 25% water, Sabet. (2016).

## 2 Anisotropic linear-elastic models of cortical bone

Although in reality bone-elastic tissue exhibits visco-elastic behavior, both in mechanical tests at low velocities and in the numerical analysis of stress and deformation state, it is considered, in an acceptable approximation, an anisotropic solid with a linear-elastic behavior, Katz (2008).

### 2.1 Tensions and deformations

The state of tension is known at a point P of a solid if the voltages that act on three orthogonal planes that pass through this point are known. In Figure 4, these are represented by even the coordinate planes of the orthogonal Cartesian system  $x_1x_2x_3$ .

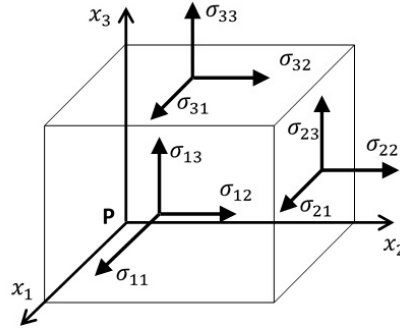


Figure 4: The state of tension at a point of a required solid

In other words, the voltage state at point P is defined by the voltage tensor with, a second-order tensor that can be represented by the array of:

$$\sigma = [\sigma] = \begin{bmatrix} \sigma_{11} & \sigma_{12} & \sigma_{13} \\ \sigma_{21} & \sigma_{22} & \sigma_{23} \\ \sigma_{31} & \sigma_{32} & \sigma_{33} \end{bmatrix} \quad (1)$$

where the tensions are normal tensions, and tensions are shear stresses (or tensile stresses). Tensions on the lines of this array act in the planes on which the coordinate

axes are normal. From the equilibrium conditions of the volume element illustrated in Figure 4 it is demonstrated that the voltage tensor is a symmetric tensor (i.e.):

$$\sigma = \begin{bmatrix} \sigma_{11} & \sigma_{12} & \sigma_{13} \\ \sigma_{21} & \sigma_{22} & \sigma_{23} \\ \sigma_{31} & \sigma_{32} & \sigma_{33} \end{bmatrix} = \begin{bmatrix} \sigma_1 & \sigma_6 & \sigma_5 \\ \sigma_6 & \sigma_2 & \sigma_4 \\ \sigma_5 & \sigma_4 & \sigma_3 \end{bmatrix} \quad (2)$$

In relation (2) the notation contraction is used, by the rule:

$$\alpha = i, \text{pentru } i = j; \alpha = 9 - i - j, \text{pentru } i \neq j \quad (3)$$

The contraction of the notation defined by the rule (3) makes it possible to represent the voltage tensor through the matrix of the column:

$$\{\sigma\} = \begin{Bmatrix} \sigma_1 \\ \sigma_2 \\ \sigma_3 \\ \sigma_4 \\ \sigma_5 \\ \sigma_6 \end{Bmatrix} \quad (4)$$

A certain point  $P$  of the solid required will move to  $P'$ , the travel vector (a first-order tensor) being defined by the three components according to the coordinate axes:

$$u = u_i = (u_1, u_2, u_3), \quad i = 1, 2, 3 \quad (5)$$

In order to study the state of deformation of a solid-called Lagrange strain Tensor is defined:

$$L_{ij} = \frac{1}{2} (u_{i,j} + u_{j,i} + u_{k,i}u_{k,j}) \quad (5)$$

where is the deformation gradient, Sadd (2014):

$$u_{i,j} = \frac{\partial u_i}{\partial x_j}$$

(6)

In the field of small deformations, ie, the second order term is neglected, and the deformation tensor it is:

$$\varepsilon = \varepsilon_{ij} = \frac{1}{2} (u_{i,j} + u_{j,i}) \quad (7)$$

Specific linear deformations (or specific lengths for) expressing elongation per unit of length:

$$\varepsilon_{11} = \frac{\partial u_1}{\partial x_1} = \varepsilon_1; \quad \varepsilon_{22} = \frac{\partial u_2}{\partial x_2} = \varepsilon_2; \quad \varepsilon_{33} = \frac{\partial u_3}{\partial x_3} = \varepsilon_3 \quad (8)$$

and specific angular deformations (or specific glides for) measures the change of right angles between two orthogonal directions:

$$\begin{aligned} 2\varepsilon_{12} = 2\varepsilon_{21} &= \left( \frac{\partial u_1}{\partial x_2} + \frac{\partial u_2}{\partial x_1} \right) = \varepsilon_6; \\ 2\varepsilon_{23} = 2\varepsilon_{32} &= \left( \frac{\partial u_2}{\partial x_3} + \frac{\partial u_3}{\partial x_2} \right) \varepsilon_4; \\ 2\varepsilon_{31} = 2\varepsilon_{13} &= \left( \frac{\partial u_3}{\partial x_1} + \frac{\partial u_1}{\partial x_3} \right) = \varepsilon_5. \end{aligned} \quad (9)$$

In the relations (8) and (9) the same notation shrinkage was used. The deformation tensor is a symmetric tensor of the second order that can be represented in the matrix form:

$$\varepsilon = [\varepsilon] \begin{bmatrix} \varepsilon_{11} & \varepsilon_{12} & \varepsilon_{13} \\ \varepsilon_{21} & \varepsilon_{22} & \varepsilon_{23} \\ \varepsilon_{31} & \varepsilon_{32} & \varepsilon_{33} \end{bmatrix} = \begin{bmatrix} \varepsilon_1 & \frac{\varepsilon_6}{2} & \frac{\varepsilon_5}{2} \\ \frac{\varepsilon_6}{2} & \varepsilon_2 & \frac{\varepsilon_4}{2} \\ \frac{\varepsilon_5}{2} & \frac{\varepsilon_4}{2} & \varepsilon_3 \end{bmatrix} \quad (10)$$

Geometric representation of deformations in the plane is illustrated in Figure 5, the approach being similar in the coordinate planes and  $x_2x_3$  and  $x_3x_1$ .

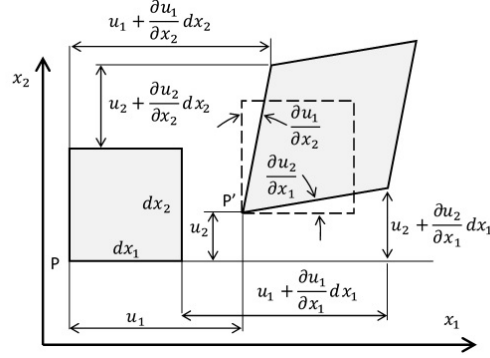


Figure 5: Deformation state

The connection between the voltage tensor and the deformation tensor is achieved with the aid of the elasticity tensor which contain our parameters of material:

$$\sigma = C_\varepsilon \tag{11}$$

or

$$\sigma_{ij} = C_{ijkl} \varepsilon_{kl} \tag{12}$$

Therefore, for a material with linear-elastic behavior, the writing of the constitutive equations (Hooke's law) is based on the hypothesis that each component of the voltage tensor is expressed by a linear combination of all the components of the deformation tensor. Tensor elasticity is a tensor of order 4 which contains, in general, 81 components ( ). Because voltage and strain tensors are symmetrical tensors:

$$\sigma_{ij} = \sigma_{ji}, \quad \varepsilon_{ij} = \varepsilon_{ji}, \tag{13}$$

tensor elasticity meets conditions, Barbero (2008) and Saddam (2014):

$$C_{ijkl} = C_{jikl} = C_{ijlk} = C_{jilk} \tag{14}$$

Thus, the number of independent components decreases from 81 to 36, and the elasticity tensor can be represented by a matrix, the constitutive equations (12) becoming in the matrix form, by the contraction of the notation:

$$\begin{pmatrix} \sigma_1 \\ \sigma_2 \\ \sigma_3 \\ \sigma_4 \\ \sigma_5 \\ \sigma_6 \end{pmatrix} = \begin{bmatrix} C_{11} & C_{12} & C_{13} & C_{14} & C_{15} & C_{16} \\ C_{21} & C_{22} & C_{23} & C_{24} & C_{25} & C_{26} \\ C_{31} & C_{32} & C_{33} & C_{34} & C_{35} & C_{36} \\ C_{41} & C_{42} & C_{43} & C_{44} & C_{45} & C_{46} \\ C_{51} & C_{52} & C_{53} & C_{54} & C_{55} & C_{56} \\ C_{61} & C_{62} & C_{63} & C_{64} & C_{65} & C_{66} \end{bmatrix} \begin{pmatrix} \varepsilon_1 \\ \varepsilon_2 \\ \varepsilon_3 \\ \varepsilon_4 \\ \varepsilon_5 \\ \varepsilon_6 \end{pmatrix} \quad (15)$$

where are coefficients of elasticity, Boresi et al. (1993). Explaining the components of the stress tensor by the specific deformation energy derivatives according to the components of the deformation tensor, it is demonstrated that the number of independent elastic coefficients is reduced from 36 to 21 for a linear-elastic anisotropic material, Boresi et al. (1993). Thus, the constitutive equations (15), in the matrix form, become:

$$\begin{pmatrix} \sigma_1 \\ \sigma_2 \\ \sigma_3 \\ \sigma_4 \\ \sigma_5 \\ \sigma_6 \end{pmatrix} = \begin{bmatrix} C_{11} & C_{12} & C_{13} & C_{14} & C_{15} & C_{16} \\ C_{21} & C_{22} & C_{23} & C_{24} & C_{25} & C_{26} \\ C_{31} & C_{32} & C_{33} & C_{34} & C_{35} & C_{36} \\ C_{41} & C_{42} & C_{43} & C_{44} & C_{45} & C_{46} \\ C_{51} & C_{52} & C_{53} & C_{54} & C_{55} & C_{56} \\ C_{61} & C_{62} & C_{63} & C_{64} & C_{65} & C_{66} \end{bmatrix} \begin{pmatrix} \varepsilon_1 \\ \varepsilon_2 \\ \varepsilon_3 \\ \varepsilon_4 \\ \varepsilon_5 \\ \varepsilon_6 \end{pmatrix} \quad (16)$$

resulting in the elasticity matrix is symmetrical. Hooke's law (16) is often expressed using the matrix of compliance, which is the reverse matrix of elasticity, Barbero (2008):

$$\begin{pmatrix} \varepsilon_1 \\ \varepsilon_2 \\ \varepsilon_3 \\ \varepsilon_4 \\ \varepsilon_5 \\ \varepsilon_6 \end{pmatrix} = \begin{bmatrix} S_{11} & C_{12} & S_{13} & C_{14} & S_{15} & C_{16} \\ S_{21} & C_{22} & S_{23} & C_{24} & S_{25} & C_{26} \\ S_{31} & C_{32} & S_{33} & C_{34} & S_{35} & C_{36} \\ S_{41} & C_{42} & S_{43} & C_{44} & S_{45} & C_{46} \\ S_{51} & C_{52} & S_{53} & C_{54} & S_{55} & C_{56} \\ S_{61} & C_{62} & S_{63} & C_{64} & S_{65} & C_{66} \end{bmatrix} \begin{pmatrix} \sigma_1 \\ \sigma_2 \\ \sigma_3 \\ \sigma_4 \\ \sigma_5 \\ \sigma_6 \end{pmatrix} \quad (17)$$

### 3 The linear elastic orthotropic and that of cortical bone

A material with three mutually orthogonal planes of symmetry and that are called orthotropic. The most well-known examples are wood with cylindrical orthotropy and unidirectional fiber composites with a Cartesian orthotropy, Barbero (2008). The model of the orthotropic material was used by Van Buskirk and Ashman (1981) to characterize the anisotropy of the cortical tissue. Their suggestion is based on experimental observations that the elastic properties of the tibia and human femur are different in the radial and circumferential directions of the transversal section (normal on the longitudinal axis of the bone). Conveniently, in Fig. 6 the coordinate planes are even the symmetry planes of the material.

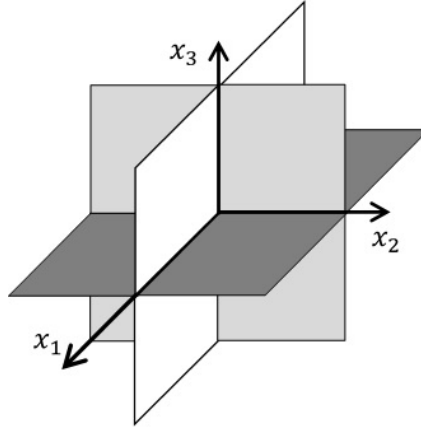


Figure 6: The planes of symmetry for an orthotropic material acid, Sadd (2014)

From the condition of symmetry to plan it follows that the following coefficients of elasticity are canceled, Barbero (2008) and Sadd (2014):

$$C_{i4} = C_{i5} = C_{46} = C_{56} = 0 \quad (i = 1, 2, 3) \quad (18)$$

Symmetry towards the plan leads to the following condition:

$$C_{16} = C_{26} = C_{36} = C_{45} = 0 \quad (19)$$

and the symmetry towards the plan is the result of the other two, without making any further changes to the elastic matrix.

Therefore, in the case of an orthotropic matrix the elasticity matrix will have 9 independent coefficients that characterize the behavior of such material. The constituent equations (16) and (17) in the matrix form are simplified as follows:

$$\begin{pmatrix} \sigma_1 \\ \sigma_2 \\ \sigma_3 \\ \sigma_4 \\ \sigma_5 \\ \sigma_6 \end{pmatrix} = \begin{bmatrix} C_{11} & C_{12} & C_{13} & 0 & 0 & 0 \\ C_{21} & C_{22} & C_{23} & 0 & 0 & 0 \\ C_{31} & C_{32} & C_{33} & 0 & 0 & 0 \\ 0 & 0 & 0 & C_{44} & 0 & 0 \\ 0 & 0 & 0 & 0 & C_{55} & 0 \\ 0 & 0 & 0 & 0 & 0 & C_{66} \end{bmatrix} \begin{pmatrix} \varepsilon_1 \\ \varepsilon_2 \\ \varepsilon_3 \\ \varepsilon_4 \\ \varepsilon_5 \\ \varepsilon_6 \end{pmatrix} \quad (20)$$

respectively

$$\begin{pmatrix} \sigma_1 \\ \sigma_2 \\ \sigma_3 \\ \sigma_4 \\ \sigma_5 \\ \sigma_6 \end{pmatrix} = \begin{bmatrix} S_{11} & S_{12} & S_{13} & 0 & 0 & 0 \\ S_{21} & S_{22} & S_{23} & 0 & 0 & 0 \\ S_{31} & S_{32} & S_{33} & 0 & 0 & 0 \\ 0 & 0 & 0 & S_{44} & 0 & 0 \\ 0 & 0 & 0 & 0 & S_{55} & 0 \\ 0 & 0 & 0 & 0 & 0 & S_{66} \end{bmatrix} \begin{pmatrix} \varepsilon_1 \\ \varepsilon_2 \\ \varepsilon_3 \\ \varepsilon_4 \\ \varepsilon_5 \\ \varepsilon_6 \end{pmatrix} \quad (21)$$

Matrix of Compliance was first deployed using the elastic properties of the experimentally determined material, as follows:

$$[S] = \begin{bmatrix} \frac{1}{E_1} & -\frac{\nu_{21}}{E_2} & -\frac{\nu_{31}}{E_3} & 0 & 0 & 0 \\ -\frac{\nu_{12}}{E_1} & \frac{1}{E_2} & -\frac{\nu_{32}}{E_3} & 0 & 0 & 0 \\ -\frac{\nu_{13}}{E_1} & -\frac{\nu_{23}}{E_2} & \frac{1}{E_3} & 0 & 0 & 0 \\ 0 & 0 & 0 & \frac{1}{G_{23}} & 0 & 0 \\ 0 & 0 & 0 & 0 & \frac{1}{G_{13}} & 0 \\ 0 & 0 & 0 & 0 & 0 & \frac{1}{G_{12}} \end{bmatrix} \quad (22)$$

In (22) represents the longitudinal modulus of elasticity in the direction the symmetry of the material, is the coefficient of transverse contraction (Poisson's coefficient) defined as the ratio of specific lengths when applying normal tension, and is the transverse elastic modulus in the plane. An orthotropic material is characterized by a set of 9 independent elastic constants, out of a total of 12, due to the symmetry of the tensor, ie we have the following relationships fulfilled:

$$\frac{\nu_{12}}{E_1} = \frac{\nu_{21}}{E_2}, \quad \frac{\nu_{13}}{E_1} = \frac{\nu_{31}}{E_3}, \quad \frac{\nu_{23}}{E_2} = \frac{\nu_{32}}{E_3}$$

(23)

Also, the coefficients of the elastic matrix can be expressed by the elastic constants of the material, taking into account the relationship. Thus, Christmas, etc. (2018):

$$C_{11} = \frac{1 - \nu_{23}\nu_{32}}{E_2 E_3 \Delta}, \quad C_{12} = \frac{\nu_{21} + \nu_{31}\nu_{23}}{E_2 E_3 \Delta} = \frac{\nu_{12} + \nu_{32}\nu_{13}}{E_1 E_3 \Delta}$$

$$C_{13} = \frac{\nu_{31} + \nu_{21}\nu_{32}}{E_2 E_3 \Delta} = \frac{\nu_{13} + \nu_{12}\nu_{23}}{E_1 E_2 \Delta}, \quad C_{22} = \frac{1 - \nu_{13}\nu_{31}}{E_1 E_3 \Delta}$$

$$C_{23} = \frac{\nu_{32} + \nu_{12}\nu_{31}}{E_1 E_3 \Delta} = \frac{\nu_{23} + \nu_{21}\nu_{13}}{E_1 E_2 \Delta}, \quad C_{33} = \frac{1 - \nu_{12}\nu_{21}}{E_1 E_2 \Delta}$$

$$C_{44} = G_{23}, \quad C_{55} = G_{13}, \quad C_{66} = G_{12}$$

(24)

where

$$\Delta = \frac{1 - \nu_{12}\nu_{21} - \nu_{23}\nu_{32} - \nu_{31}\nu_{13} - \nu_{21}\nu_{32}\nu_{13} - \nu_{12}\nu_{23}\nu_{31}}{E_1 E_2 E_3}$$

(25)

Relationships (23) and (25) represent restrictions that experimentally determined elastic properties have to meet. Also, from (24) and (23) the restriction follows:

$$1 - \nu_{ij}\nu_{ji} > 0, \quad 0 < \nu_{ij} < \sqrt{\frac{E_i}{E_j}} \quad (i, j = 1, 2, 3; i \neq j)$$

(26)

## 4 The isotropic cross-sectional arthroplasty of the cortical bone

The transverse-isotropic material has an axis of symmetry, and consequently the planes containing this axis are symmetry planes (see Figure 7, the symmetry axis is). The transversal-isotropic model was used by Lang (1969), Katz and Ukraincik (1971) and Yoon and Katz (1976) to characterize cortical bone anisotropy.

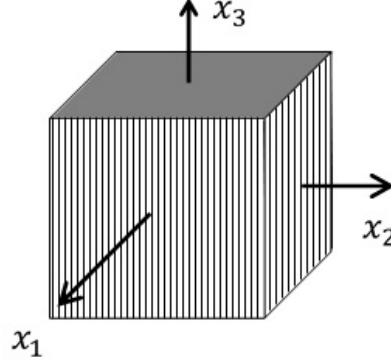


Figure 7: Symmetry axis for a transverse-isotropic material, Sadd (2014)

A transversal-isotropic material is characterized by a set of 5 independent elastic constants with the elastic matrix:

$$\begin{bmatrix} C_{11} & C_{12} & C_{13} & 0 & 0 & 0 \\ C_{12} & C_{11} & C_{13} & 0 & 0 & 0 \\ C_{13} & C_{13} & C_{33} & 0 & 0 & 0 \\ 0 & 0 & 0 & C_{44} & 0 & 0 \\ 0 & 0 & 0 & 0 & C_{44} & 0 \\ 0 & 0 & 0 & 0 & 0 & \frac{C_{11}-C_{12}}{2} \end{bmatrix}$$

(27)

and relationships between elastic properties, Katz (2008):

$$E_1 = E_2, \nu_{12} = \nu_{21}, G_{12} = \frac{E_1}{2(1 + \nu_{12})}$$

$$\nu_{31} = \nu_{32} = \nu_{13} = \nu_{23}, G_{23} = G_{31}$$

(28)

## 5 Analysis numerical propagation of a cracks into the cortical bone (how mixed I-II)

The method of the finite element (MEF) is used into the biomechanics for The study TAD's behavior Mechanical Tissue bone, and examples are numerous: analysis st country voltage of femur human, Basuša (1985 ); prediction breaking bone fem,

ral, Marco et al. (2018); estimate property mechanical of the vertebral bone, Brown et al. (2014); micrometric scale modeling of cortical bone breakage, Idkaidek and Jasiuk (2016), Li et al. (2013).

The conditions for starting the break cortical bone, for call into the module mixed I-II, is studied numeral into the continuation on The bending specimens NTI symmetric into the four points (AFPB - Asymmetric Four Point Bendspecimen )

### 5.1 Geometry of the AFPB specimen

The AFPB test was used in the mixed I-II breakdown study for ceramic materials, Suresh et al. (1990), granite, Razavi et al. (2017), alumina-PMMA, Marsavina, and others. (2013) or cortical bone, Zimmermann et al. (2009).

Geometry of the AFPB specimen and how to apply for the pattern used in this study are presented into the Figure 8, with thickness.

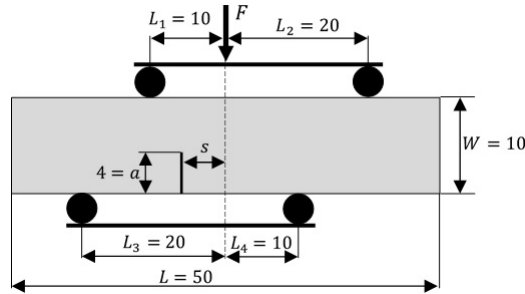


Figure 8: The AFPB test

Force is applied at a distance to the crack length (see Figure 8). Thus, the request into this plan (rift) is bending with force cutting efforts calculating with the relationships:

$$T = F \frac{L_2 - L_1}{L}, \quad M(s) = Ts \quad (29)$$

Into the case, the crack is produced only shear pure, obtaining a request in Mode II. Changing distance of the direction of force action and the crack plane, that is, for, is achieved applications into the module.  $C$  mixed ombi nation from Modules I and II are characterized through parameter to dimensional:

$$M^e = \frac{2}{\pi} \arctan \left( \frac{k_1}{k_{11}} \right)$$

(30)

The relationship (30), and the voltage for mode are the factors of intensity I of the request, so mode II, expressions of the form, Suresh et al. (1990)

$$K_1 = \varsigma \sqrt{\pi a} Y_1(a/W) = \frac{6M}{W^2 t} \sqrt{\pi a} Y_1(a/W) = 6\tau \frac{s}{W} \sqrt{\pi a} Y_1(a/W)$$

$$K_{II} = \tau \sqrt{\pi a} Y_1(a/W)$$

(31)

Some functions depend on the report. Into the configuration, we have obtained superior values to about the results published by Suresh and others. (1990). Tensions and are produced by the bending and shearing requirements in the crack plane.

Mode I application ( ) is not obtained in antisymmetric configuration your presence into the Figure 8 because for any parameter value. Throughout, in the skeleton, a symmetric configuration is involved and i, for the epoch in the study.

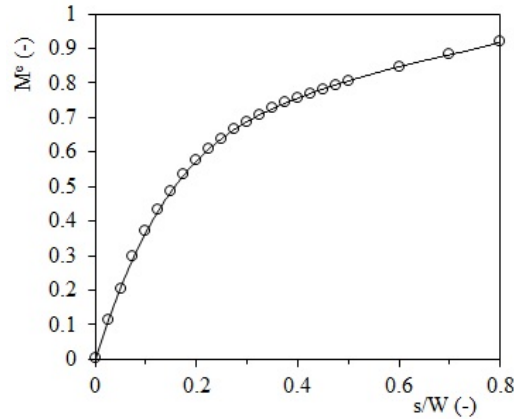


Figure 9: The variation of the M parameter is based on the position of the crack plane

Figure 9 is presented combination from Module I and Module II, in depending on the report, for:

## 5.2 Numerical Determination of Breaking Mechanics Parameters

To determine the fracture mechanics parameters at the crack tip, the finite element method was implemented in the FRANC2D / L 1.5 software developed at Cornell University, Wawrzynek (1991). Two types of isotropic and transverse isotropic

materials were studied comparatively. The working steps are further described for the AFPB sample shown in Figure 8.

The geometric modeling and meshing is performed with the CASCA pre-processor. The specimen geometry is made up of three sub-regions, especially because onvenabil for meshing (*G e ometry* menu commands *Get Line LinesConnected*). To control meshing parameters, such as number of elements and spacing along one side, the *No. of segments* and *Ratio* commands in the *Subdivide* menu are used (see Figure 10).



Figure 10: Determining the number of elements and spacing along the sides

Mesh Mesh specimen is carried out by selecting the menu items Q8 and technical quadratic bilinear 4side type recommended for the rectangular regions of the same apple nodes not on opposite sides (Figure 11).

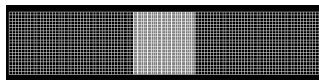


Figure 11: Specimen design

After completion meshed country save a CASCA file (e.g. *afpb.csc*, *Write* command) that can change then. Also, further analysis is saved a *FRANC2D / L* file, for example *afpb.inp* (*Write Mesh* command), file which import computing model.

The calculation of the number of mechanical parameters break with the method element *Efe ctuează* program is finished *FRANC 2D / L*.

Stage Understanding-processing assume the establishment conditions in which it is settled application: the type of problem, and material properties the limiting conditions.

Thickness taking account the specimen, equal with it was considered a matter of state plane stress (*Pre-Process* menu, submenu *Problem Type*, *Plane Stress* command).

Defined two material is first a behavior isotropic, and the second with a transversely isotropic behavior, properties, and *Burstein Reilly (1975)* considering specimen taken into the over axis The main material (*Pre-Process* menu, submenu *Material / New Mat*, *ElastIso* command / *ElastOrth*), through cancellation travel appropriate (*Pre-Process* menu, submenu *fixity*, *Ind Fix* command), and the load applied

applied applying the specimen (Pre-Process menu, submenu Loads, Load command Point).

Into the Processing steps and post processing is carried out analyze the stress and strain (Analysis menu, submenu Linear, Stiff direct command) and the viewing Results (Post-Process menu, submenu Contour command Stress / Strain). The program performs the linear-elastic analysis of the stress state using the direct elimination method (Gauss Removal Method).

Analyze parameters of mechanics breaking for the AFPB sample is being initiated through introduction of a edge cracks, whose sides are unencumbered (Modify menu, submenu New Crack, Non-Cohesive and EdgeCrack commands). Specify the edge node leading to the crack, the crack tip and the minimum number of finite elements on the crack length. At the tip of the crack, the program introduces a rosette consisting of 8 singular finite elements for modeling singularity, Figure 12.

For that a new one has emerged s STRUCTURE (specimen cracked), is carried out nine analysis of the state of tension and is calculated mechanical parameters Breaking: the angle the crack extension and the stress intensity factors and i. The FRANC2D / L program uses some techniques for calculation of stress intensity factors: extrapolation displacements, integral, the extension virtual crack. The method of extrapolation travel was used for evaluation stress intensity factors and in simulation of crack propagation on AFPB specimens (Post-Process menu, submenu fraction Mech, DSPCorr SIF / SIF History commands).

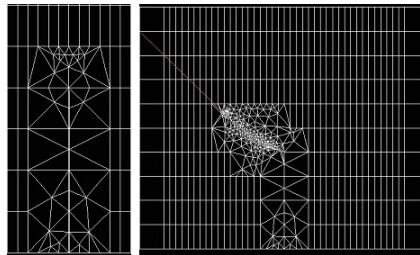


Figure 12: Starting the edge crack detail and propagating it in the II mode of application; isotropic material, increment 0.2 mm, 15 steps

Propagation crack is performed into the FRANC2D / L through standard technique or through technique automatic . Direction of propagation and the position new the peak of the crack is determined on the base of three initiation criteria into the module mixed, and namely: criterion blood circumfer Entiat maximum, criterion energy ie specific deformity minimum, respectively, the criterion ie force and maximum extension of the crack. After the establishment increment and a dir ECTI extension FIS hatred finite elements positioned along the path are removed and a

surface polygonal temporary intended for re-use mesh it is generated . Fissure initial It is exile nLet into the nine position of the tip and it is brought a rosette consisting of 8 triangular finite elements isobar a metric singular . Surface in the neighborhood ii crack it is discretized automatic. Into the Figure 12 is this t the outcome spread crack for an increment equal to and 15 consecutive steps using automatic technique (Modify menu, submenus Move Crack / Automatic, the Propagate command).

## 6 Results and conclusions

Trajectories crack, for the two materials, in Module I and Request Module II are presented into the Figures 13 and 14. Conditions critical crack extension, as the critical opening angle, are different for the two materials; same observation results and Figure 15, where for three stress situations (how I, how mixed I + II and module II) results number are represented into the compared to the solution criterion blood circumferential maximum (MTS criterion), Erdogan and Sih (1963). Validation results number and determination force critical crack extension assume Tests mechanical on cortical bone.

Also, it is proposed, in studiu a future use the XFEM method , implemented into the ABAQUS program, for modeling spread cracks into the case materials anisotrope.

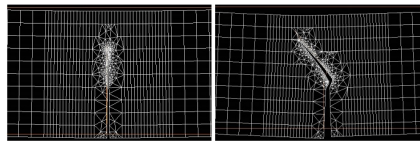


Figure 13: Fracture trajectory for load mode I (left - isotropic material, right - isotropic cross-sectional material)

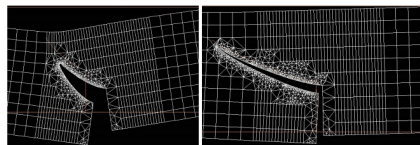


Figure 14: Fracture trajectory for load mode II (left - isotropic material, right - isotropic cross-sectional material)

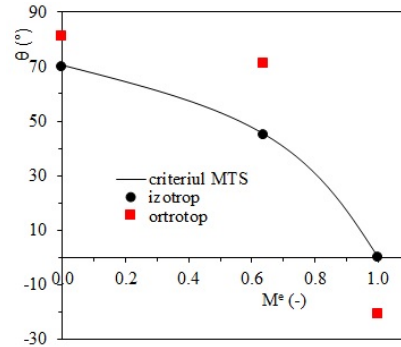


Figure 15: Critical angle of initiation to crack extension

## References

- [1] R. Baptista, A. Almeida, V. Infante (2016), Micro-crack propagation on a biomimetic bone-like composite material studied with the extended finite element method, *Procedura Structural Integrity* 1, 018-025.
- [2] E.J. Barbero (2008), *Finite Element Analysis of Composite Materials*, CRC Press, Taylor and Francis Group.
- [3] P.K. Basu, A. G. Beall, D. J. Simmons, M. W. Vannier (1985), 3-D femoral stress analysis using CT scans and p-version FEM, *Biomaterials, Medical Devices, and Artificial Organs* 13, 163-186.
- [4] A. P. Boresi, R. J. Schmidt, O. M. Sidebottom (1993), *Advanced Mechanics of Materials*, 5th edition, John Wiley and Sons Ltd.
- [5] K. R. Brown, S. Tarsuslugil, V. N. Wijayathunga, R. K. Wilcox (2014), Comparative finite element analysis: a single computational modeling method can estimate the mechanical properties of porcine and human vertebrae, *Journal of the Royal Society Interface* 11, 20140186.
- [6] E. M. Christmas, A. Rabaea, M. F. Popa, C. I. Mihailov (2018), Crack propagation in the human bone. Mode I of Fracture, *Annals of Science of "Ovidius" University Constanta* 26, 59-70.
- [7] F. Erdogan, G. C. Sih (1963), On the crack extension in plates by plane loading and transverses shear, *Journal of Basic Engineering, Transactions of ASME* 85, 519-525.

- [8] A. Idkaidek, I. Jasiuk (2016), Cortical bone fracture analysis using XFEM-case study, *International Journal for Numerical Methods in Biomedical Engineering*, e02809.
- [9] J. L. Katz, K. Ukraincik (1971), On the thean isotropic elastic properties of hydro xyapatite, *Journal of Biomechanics* 4, 221-227.
- [10] J. L. Katz (2008), Mechanics of hard tissue, in: Peterson DR and Bronzino JD (ed.), *Biomechanics. Principles and Applications*, 9-20, CRC Press, Francis and Taylor Group.
- [11] J .H. Kim, D. Kim, M. G. Lee (2013), Mechanics of cellular materials and its applications in: S. Li and D. Qian (ed.), *Multi-scale Simulations and Mechanics of Biological Materials*, 411-434, John Wiley and Sons Ltd.
- [12] S. B. Lang (1969), Elastic coefficients of animal bone, *Science* 165, 287-288.
- [13] S. Li, A. Abdel- Wahab, E. Demirci, V. V. Silberschmidt (2013), Fracture process in cortical bone: X-FEM analysis of micro-structured models, *International Journal of Fracture* 184, 43-55.
- [14] M. Marco, E. Giner, R. Larrainzar-Garijo, J. R. Caeiro, M. H. Miguélez (2018), Modeling of femoral fracture using finite element procedures, *Engineering Fracture Mechanics* 196, 157-167.
- [15] L. Marsavina, T. Sadowski, M. Kneć (2013), Crack-propagation paths in four-pointbend Aluminum-PMMA, *Engineering Fracture Mechanics* 108, 139-151.
- [16] S. M. J. Razavi, M. R. M. Aliha, F. Berto (2017), Applying a strain energy density criterion to obtain the mixed mode fracture load of granite rock tested with the cracked asymmetric four-point bend specimens, *Theoretical and Applied Fracture Mechanics*, In press, corrected proof, Available online 8 July 2017.
- [17] D. T. Reilly, A. H. Burstein (1975), The elastic and ultimate properties of compact bone tissue, *Journal of Biomechanics* 8, 393-405.
- [18] F. A. Sabet, A. R. Najafi, E. Hamed, I. Jasiuk (2016), Modeling of bone fracture and strength at different length scales: a review, *Interface Focus* 6, 20150055.
- [19] M. H. Sadd (2014), *Elasticity: Theory, Applications and Numerical* 3 rd Edition, Elsevier.
- [20] S. Suresh, C. F. Shih, A. Morrone, N. P. O'Dowd (1990), Mixed-mode fracture toughness of ceramic materials, *Journal of the American Ceramic Society* 73, 1257-1267.

- [21] D. Taylor (2010), Why Do not Your Bones not made of Steel?, *Materials Today* 13, 6-7.
- [22] W. C. Van Buskirk, R. B. Ashman R.B. (1981), The elastic moduli of bone, in: Cowin S.C. (ed.), *Mechanical Properties of Bone AMD*, vol 45, 131-143, American Society of Mechanical Engineers.
- [23] P. A. Wawrzynek (1991), Discrete modeling of crack propagation: theoretical aspects and implementation issues in two and three dimensions, PhD Thesis, Cornell University, Ithaca.
- [24] E. A. Zimmermann, M. E. Launey, H. D. Barth, R. O. Ritchie (2009), Mixed-mode fracture of human cortical bone, *Biomaterials* 30, 5877-5884.
- [25] H. S. Yoon, J. L. Katz (1976), Ultrasonic wave propagation in human cortical bone: I. Theoretical considerations of hexagonal symmetry, *Journal of Biomechanics* 9, 407-412.

Ioana Ramona Iosif  
Department of Mathematics,  
Politehnica University of Timisoara,  
P-ta Victoriei 2, 300006, Timisoara, ROMANIA  
E-mail: ioana\_ramo@yahoo.com

## A GENERALIZATION OF YOUNG’S THEOREM AND SOME APPLICATIONS

Sorin LUGOJAN, Loredana CIURDARIU

### Abstract

A generalization of classical Young’s inequality for non-convex linear combinations is given, followed by applications to functionals. <sup>1</sup>

Keywords and phrases: *Young’s inequality, isotonic linear functional*

## 1 Introduction

William Henry Young published in 1912 an inequality which extends the well known relation between arithmetic and geometric means. Now, that is called Young’s inequality:

$$x^\alpha y^\beta \leq \alpha x + \beta y,$$

for any  $x, y \geq 0$  and any positive  $\alpha, \beta$  such that  $\alpha + \beta = 1$ .

In the last years, Young’s inequality reappeared as a research theme and many improved inequalities, originated from that, were published by authors as: T. Ando, F. Kittaneh and Y. Manasrah, M. Tominaga, S. Furuichi, N. Minculete, J. M. Aldaz, S. S. Dragomir and O Hirzallah, see [2, 13, 14, 5, 10, 9, 11, 17, 1, 8, 7] and the references therein. T. Ando, O. Hirzallah and F. Kittaneh and Y. Manasrah used it for matrices and also S. Furuichi and N. Minculete and S. S. Dragomir used it for operators. Also W. Liao, J. Wu and J. Zhao and S. Manjeani generalized this inequality in recent years.

As a common feature of these new inequalities is the relation  $\alpha + \beta = 1$ .

In the followings we are going to state and prove inequalities beyond that condition.

---

<sup>1</sup>MSC (2010): 26D15

## 2 Generalization of Young's theorem

**Theorem 2.1** (a) In case  $\alpha + \beta > 1$ , and  $\alpha \in (0, 1)$ , then

$$\alpha x + \beta y > x^\alpha y^\beta,$$

for all  $x, y > 0$ .

(b) In case  $\alpha + \beta = 1$ , and  $\alpha, \beta \geq 0$ , then

$$\alpha x + \beta y \geq x^\alpha y^\beta,$$

for all  $x, y \geq 0$ .

(c) In case  $\alpha < 0$ ,  $\beta < 0$ , then

$$\alpha x + \beta y < x^\alpha y^\beta,$$

for all  $x, y > 0$ .

*Proof.* Let's find the extremes of the mapping

$$f(x, y) = \alpha x + \beta y - x^\alpha y^\beta,$$

for  $x, y > 0$ ,  $\alpha, \beta \in \mathbf{R}_*$ .

The stationary points of  $f$  are given by the system

$$\begin{cases} \frac{\partial f}{\partial x} = \alpha - \alpha x^{\alpha-1} y^\beta = 0 \\ \frac{\partial f}{\partial y} = \beta - \beta x^\alpha y^{\beta-1} = 0 \end{cases} .$$

That system is equivalent to the following one:

$$\begin{cases} x^{\alpha-1} y^\beta = 1 \\ x^\alpha y^{\beta-1} = 1 \end{cases}$$

which gives, by division:  $\frac{y}{x} = 1$ , hence  $x = y$ , and the unique stationary point of  $f$  is  $(1, 1)$ . The hessian matrix of  $f$  is:

$$\begin{aligned} (Hf)(x, y) &= - \begin{pmatrix} \alpha(\alpha-1)x^{\alpha-2}y^\beta & \alpha\beta x^{\alpha-1}y^{\beta-1} \\ \alpha\beta x^{\alpha-1}y^{\beta-1} & \beta(\beta-1)x^\alpha y^{\beta-2} \end{pmatrix} = \\ &= -x^{\alpha-2}y^{\beta-2} \begin{pmatrix} \alpha(\alpha-1)y^2 & \alpha\beta xy \\ \alpha\beta xy & \beta(\beta-1)x^2 \end{pmatrix}. \end{aligned}$$

The minor determinants  $\Delta_1, \Delta_2$ , of Sylvester's theorem, have the same sign as  $d_1 = -\alpha(\alpha - 1)$ ,  $d_2 = -[\alpha\beta(\alpha - 1)(\beta - 1) - \alpha^2\beta^2] = -\alpha\beta(1 - \alpha - \beta)$ .

**1.** The point  $(1, 1)$  is a global minimum for  $f$  if  $\Delta_1, \Delta_2 > 0$ ,  $\forall x, y > 0$ , that is  $d_1, d_2 > 0$  or

$$\begin{cases} \alpha(\alpha - 1) < 0 \\ \alpha\beta(1 - \alpha - \beta) < 0 \end{cases} . \quad (1)$$

**1.1** By the first inequality of (1), if  $\alpha > 0$ , then  $\alpha - 1 < 0$ ,  $\alpha < 1$ , hence  $\alpha \in (0, 1)$ . Here, we may have two cases, depending on the second inequality of (1):

**1.1.1** If  $\beta > 0$ , then  $1 - \alpha - \beta < 0$ ,  $\alpha + \beta > 1$ , and

$$f(x, y) \geq f(1, 1) = \alpha + \beta - 1 > 0, \forall x, y > 0,$$

hence  $f(x, y) > 0$  or  $\alpha x + \beta y > x^\alpha y^\beta$ , which is the statement (a).

**1.1.2** If  $\beta < 0$ , then  $1 - \alpha - \beta > 0$ ,  $\alpha + \beta < 1$ , and

$$f(x, y) \geq f(1, 1) = \alpha + \beta - 1 < 0, \forall x, y > 0.$$

By that we have no conclusion.

**1.2** If  $\alpha < 0$ , then  $\alpha - 1 > 0$ ,  $\alpha > 1$ , and that is impossible.

**2.** The point  $(1, 1)$  is a global maximum for  $f$  if  $\Delta_1, \Delta_2 < 0$ ,  $\forall x, y > 0$ , that is  $d_1, d_2 < 0$ , or

$$\begin{cases} \alpha(\alpha - 1) > 0 \\ \alpha\beta(1 - \alpha - \beta) > 0 \end{cases} . \quad (2)$$

**2.1** If  $\alpha > 0$ , then  $\alpha > 1$ , hence  $\alpha > 1$ .

**2.1.1** If  $\beta > 0$ , then  $1 - \alpha - \beta > 0$ ,  $\alpha + \beta < 1$ , but these three conditions are incompatible.

**2.1.2** If  $\beta < 0$ , then  $1 - \alpha - \beta < 0$ ,  $\alpha + \beta > 1$ , and

$$f(x, y) \leq f(1, 1) = \alpha + \beta - 1 > 0, \forall x, y > 0,$$

which gives no conclusion.

**2.2** If  $\alpha < 0$ , then  $\alpha - 1 < 0$ ,  $\alpha < 1$ , hence it remains that  $\alpha < 0$ .

**2.2.1** If  $\beta > 0$ , then  $1 - \alpha - \beta < 0$ ,  $\alpha + \beta > 1$ , and

$$f(x, y) \leq f(1, 1) = \alpha + \beta - 1 > 0, \forall x, y > 0,$$

and we have no conclusion.

**2.2.2** If  $\beta < 0$ , then  $1 - \alpha - \beta > 0$ ,  $\alpha + \beta < 1$ , and

$$f(x, y) \leq f(1, 1) = \alpha + \beta - 1 < 0, \forall x, y > 0,$$

hence  $f(x, y) < 0$ ,  $\forall x, y > 0$ , which is equivalent to the statement (c). The statement (b) is the classical Young's inequality.

In order to extend the previous Theorem 2.1, in the frame of functionals theory, we recall the following definition (one also may see [3], [4], [5]).

**Definition 2.2** Let  $E$  be a nonempty set and  $L$  be a linear class of real-valued functions  $f, g : E \rightarrow \mathbf{R}$  having the following properties:

(L1)  $f, g \in L$  imply  $(\alpha f + \beta g) \in L$  for all  $\alpha, \beta \in \mathbf{R}$ .

(L2)  $1 \in L$ , i.e., if  $f_0(t) = 1$ ,  $\forall t \in E$ , then  $f_0 \in L$ .

An isotonic linear functional is a functional  $A : L \rightarrow \mathbf{R}$  having the following properties:

(A1)  $A(\alpha f + \beta g) = \alpha A(f) + \beta A(g)$  for all  $\alpha, \beta \in \mathbf{R}$ ;

(A2) If  $f \in L$  and  $f(t) \geq 0$  then  $A(f) \geq 0$ .

The mapping  $A$  is said to be normalized if

(A3)  $A(1) = 1$ .

The extension of the inequality (a) of Theorem 2.1 is stated as follows:

**Theorem 2.2** Let  $A : L \rightarrow \mathbf{R}$  be an normalized isotonic linear functional. If  $f, g \geq 0$ ,  $f^\alpha g^\beta \in L$  and  $A(f), A(g) > 0$  and  $\alpha, \beta$  are real numbers so that  $\alpha + \beta > 1$ ,  $\alpha \in (0, 1)$  then the following inequality holds:

$$(\alpha + \beta)A^\alpha(f)A^\beta(g) > A(f^\alpha g^\beta). \quad (3)$$

Now, if  $f, g \geq 0$ ,  $f^\alpha g^\beta \in L$  and  $A(f), A(g) > 0$  and  $\alpha < 0$ ,  $\beta < 0$ , then

$$(\alpha + \beta)A^\alpha(f)A^\beta(g) < A(f^\alpha g^\beta), \quad (4)$$

where  $f, g : E \rightarrow \mathbf{R}$  are previous functions.

*Proof.* If we take in Theorem 2.1 (a),  $x = \frac{f}{A(f)}$ ,  $y = \frac{g}{A(g)}$  then we get,

$$\alpha \frac{f}{A(f)} + \beta \frac{g}{A(g)} > \frac{f^\alpha}{A^\alpha(f)} \frac{g^\beta}{A^\beta(g)}.$$

Now, if we take the functional  $A$  in previous inequality, we find that

$$A\left(\alpha \frac{f}{A(f)} + \beta \frac{g}{A(g)}\right) > A\left(\frac{f^\alpha}{A^\alpha(f)} \frac{g^\beta}{A^\beta(g)}\right),$$

or

$$\alpha + \beta > \frac{A(f^\alpha g^\beta)}{A^\alpha(f)A^\beta(g)},$$

or

$$(\alpha + \beta)A^\alpha(f)A^\beta(g) > A(f^\alpha g^\beta),$$

if  $\alpha + \beta > 1$ ,  $\alpha \in (0, 1)$  and  $\beta > 0$ .

For the second inequality, (4), we consider Theorem 2.1, (c) and we put  $x = \frac{f}{A(f)}$ ,  $y = \frac{g}{A(g)}$ . Then we have,

$$\alpha \frac{f}{A(f)} + \beta \frac{g}{A(g)} < \frac{f^\alpha}{A^\alpha(f)} \frac{g^\beta}{A^\beta(g)},$$

and from here, using the functional  $A$ , we obtain,

$$\alpha + \beta < \frac{A(f^\alpha g^\beta)}{A^\alpha(f)A^\beta(g)},$$

or

$$(\alpha + \beta)A^\alpha(f)A^\beta(g) < A(f^\alpha g^\beta),$$

where  $\alpha < 0$ ,  $\beta < 0$ .

Another extension of the inequality (a) of the Theorem 2.1 is the following:

**Theorem 2.3** *Let  $A, B : L \rightarrow \mathbf{R}$  be two normalized isotonic linear functionals. If  $f, g : E \rightarrow \mathbf{R}$  are so that  $f \geq 0$ ,  $g > 0$ ,  $f^\alpha g^{1-\alpha}$ ,  $f^\beta g^{1-\beta} \in L$  and  $\alpha, \beta \in \mathbf{R}$  with  $\alpha + \beta > 1$ ,  $\alpha \in (0, 1)$ ,  $\beta \in (0, 1)$ , then we have:*

$$\alpha A(f)B(g) + \beta A(g)B(f) > A(f^\alpha g^{1-\alpha})B(f^\beta g^{1-\beta}). \quad (5)$$

*Proof.* We use inequality (a) from Theorem 2.1 for  $x = \frac{f(z)}{g(z)}$ ,  $y = \frac{f(t)}{g(t)}$ , and we have:

$$\alpha \frac{f(z)}{g(z)} + \beta \frac{f(t)}{g(t)} > \frac{f^\alpha(z) f^\beta(t)}{g^\alpha(z) g^\beta(t)}.$$

Multiplying by  $g(z)g(t) > 0$  we obtain,

$$\alpha f(z)g(t) + \beta f(t)g(z) > f^\alpha(z)g^{1-\alpha}(z)f^\beta(t)g^{1-\beta}(t)$$

for any  $z, t \in E$ .

Fix  $t \in E$  and then by previous inequality we have in the order of  $L$  that

$$\alpha f g(t) + \beta f(t) g > f^\alpha g^{1-\alpha} f^\beta(t) g^{1-\beta}(t).$$

If we take now the functional  $A$  in previous inequality then we have:

$$\alpha g(t) A(f) + \beta f(t) A(g) > f^\beta(t) g^{1-\beta}(t) A(f^\alpha g^{1-\alpha}),$$

for any  $t \in E$ .

This inequality can be written in the sense of the order of  $L$  as

$$\alpha g A(f) + \beta f A(g) > f^\beta g^{1-\beta} A(f^\alpha g^{1-\alpha}),$$

and now, if we take into account the functional  $B$  in last inequality, then we obtain the desired result.

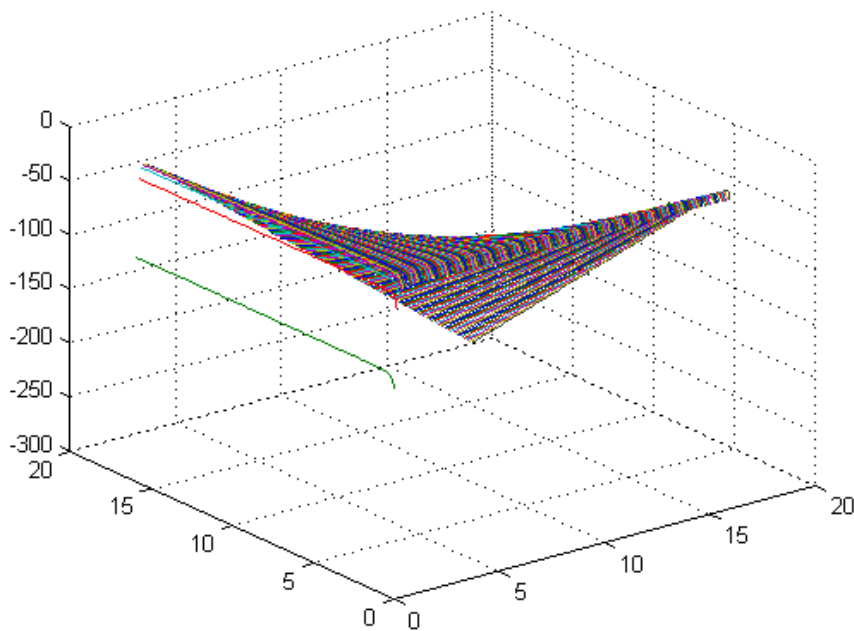


Figure 1: The graph of the function  $f(x, y) = \alpha x + \beta y - x^\alpha y^\beta$  for  $\alpha = -\frac{3}{7}$  and  $\beta = -\frac{6}{7}$

## References

- [1] Aldaz J. M., A stability version of Holder's inequality, *J. Math. Anal. Appl.* 343, 842-852, (2008).
- [2] Ando T., Matrix Young inequalities, *Oper. Theory Adv. Appl.* 75 (1995), 3338.
- [3] Andrica D. and Badea C., Gruss'inequality for positive linear functionals, *Periodica Math. Hung.*, 19, 155-167, (1998).
- [4] Anwar M., Bibi R., Bohner M., and Pecaric J., Integral Inequalities on Time Scales via the Theory of Isotonic Linear Functionals, *Abstract and Applied Analysis*, Article ID 483595, 16 pages, (2011).
- [5] Dragomir S. S., A survey of Jessen's type inequalities for positive functionals, *RGMI Res. Rep. Coll.*, 46 pp, (2011).
- [6] Dragomir S. S., A Gruss type inequality for isotonic linear functionals and applications, *RGMI Res. Rep. Coll.*, 10 pp, (2002).
- [7] Dragomir S. S., A note on Young's inequality, *RGMI Res. Rep. Coll.*, 5 pp, (2015).
- [8] Dragomir S. S., Some new reverses of Young's operator inequality, *RGMI Res. Rep. Coll.*, 12 pp, (2015).
- [9] Furuichi S., On refined Young inequalities and reverse inequalities, *Journal of Mathematical Inequalities*, **5**, 1(2011), 21-31.
- [10] Furuichi S., Minculete N., Alternative reverse inequalities for Young's inequality, *Journal of Mathematical inequalities*, **5**, 4 (2011), 595-600.
- [11] Hirzallah O., Kittaneh F., MatrixYoung's inequalities for the Hilbert-Schmidt norm, *Linear Algebra Appl.*, 308: 77-84, (2000).
- [12] Liao W., Wu J., Zhao J., New versions of reverse Young and Heinz mean inequalities with the Kantorovich constant, *Taiwanese J. Math* 19 No.2, pp. 467-479, (2015).
- [13] Kittaneh F., Manasrah Y., Reverse Young and Heinz inequalities for matrices, *Linear and Multilinear Algebra*, **59**, 9 (2011), 1031-1037.
- [14] Kittaneh F., Manasrah Y., Improved Young and Heinz inequalities for matrices, *J. Math. Anal. Appl.*, **361** (2010), 262-269.

- [15] Manjegani S., Hölder and Young inequalities for the trace of operators, *Positivity* 11 (2007), 239250.
- [16] Strang G., "Linear Algebra and its Applications" (fourth edition), Thompson Publishing House, (2006).
- [17] Tominaga M., Spect's ratio in the Young inequality, *Sci. Math. Japon.*, 55, 563-585, (2002).
- [18] Young W. H., On classes of summable functions and their Fourier series, *Proc. Royal Soc. London, Ser. A.* 87:225-229, (1912).

Sorin Lugojan and Loredana Ciurdariu  
Department of Mathematics,  
Politehnica University of Timisoara,  
P-ta. Victoriei 2, 300006, Timisoara, ROMANIA  
E-mail: sorin.lugojan@upt.ro  
E-mail: loredana.ciurdariu@upt.ro

## APPLICATIONS OF THE NON-CONVEX YOUNG’S INEQUALITY IN HILBERT SPACES

Loredana CIURDARIU, Sorin LUGOJAN

### Abstract

A generalization of classical Young’s inequality is applied for operators in Hilbert spaces. <sup>1</sup>

Keywords and phrases: *Young’s inequality, operators, separable Hilbert spaces.*

## 1 Introduction

Let  $\mathcal{B}(\mathcal{H})$  be the  $C^*$ – algebra of all bounded linear operators on a complex Hilbert space  $\mathcal{H}$ , and let  $A, B \in \mathcal{B}(\mathcal{H})$  be two positive operators.

We recall the definition of the weighted arithmetic mean of  $A$  and  $B$  denoted by  $A\nabla_\nu B$  :

$$A\nabla_\nu B = (1 - \nu)A + \nu B,$$

where  $\nu \in [0, 1]$ .

If  $A$  is invertible then the weighted geometric mean of  $A$  and  $B$ , denoted by  $A\sharp_\nu B$ , is defined by:

$$A\sharp_\nu B = A^{\frac{1}{2}} \left( A^{-\frac{1}{2}} B A^{-\frac{1}{2}} \right)^\nu A^{\frac{1}{2}}.$$

When  $\nu = \frac{1}{2}$  we notate  $A\nabla B$  and  $A\sharp B$  instead of  $A\nabla_{\frac{1}{2}} B$  and  $A\sharp_{\frac{1}{2}} B$ .

If  $A$  and  $B$  are positive invertible operators, it is well-known that:

$$A\nabla_\nu B \geq A\sharp_\nu B, \forall \nu \in (0, 1),$$

which is the operatorial version of the classical Young’s inequality, see [9]

In the followings we will give some variants of the non-convex Young’s operatorial inequality based on [10].

---

<sup>1</sup>MSC (2010): 26D15

## 2 Main results

**Proposition 2.1** *Let  $A, B$  be two positive invertible operators on  $\mathcal{H}$  so that there is an  $r > 0$  such*

$$(1 - r)B \leq A \leq (1 + r)B.$$

*Then we have:*

$$\alpha A + \beta B > B \sharp_{\alpha} A, \quad (1)$$

*for any  $\alpha, \beta$  fulfilling the conditions  $\alpha + \beta > 1, \alpha \in (0, 1)$ .*

*Moreover,*

$$\alpha A + \beta A^{\beta} > A^{\alpha + \beta^2}, \quad (2)$$

*as well as*

$$\alpha A + \beta A^{\alpha} > A^{\alpha + \alpha\beta}, \quad (3)$$

*for all  $\alpha, \beta$  checking  $\alpha + \beta > 1$  and  $\alpha \in (0, 1)$ .*

*Proof.* We take  $y = 1$  in the inequality (a) of Theorem 2.1 presented in [10] and we get  $\alpha x + \beta y > x^{\alpha}$  when  $\alpha + \beta > 1$  and  $\alpha \in (0, 1)$ .

Using the functional calculus with continuous functions of spectrum, see [1] page 8, we find out that

$$\alpha X + \beta I > X^{\alpha},$$

where  $X$  is the strictly positive operator on  $\mathcal{H}$ .

If we put instead of the operator  $X$  the strictly positive operator  $B^{-\frac{1}{2}}AB^{-\frac{1}{2}}$  we obtain

$$\alpha B^{-\frac{1}{2}}AB^{-\frac{1}{2}} + \beta I > \left( B^{-\frac{1}{2}}AB^{-\frac{1}{2}} \right)^{\alpha},$$

when  $\alpha + \beta > 1$  and  $\alpha \in (0, 1)$ .

Multiplying both sides of previous inequality by  $B^{\frac{1}{2}}$ , it results

$$\alpha A + \beta B > B^{\frac{1}{2}} \left( B^{-\frac{1}{2}}AB^{-\frac{1}{2}} \right)^{\alpha} B^{\frac{1}{2}},$$

when  $\alpha + \beta > 1$  and  $\alpha \in (0, 1)$ , which is the relation (1) of the statement.

For the second inequality considering  $y = x^{\beta} > 0$  and then  $y = x^{\alpha} > 0$  in the inequality (a) of Theorem 2.1 ([10]) we obtain

$$\alpha x + \beta x^{\beta} > x^{\alpha} y^{\beta^2}, \quad \alpha x + \beta x^{\alpha} > x^{\alpha + \alpha\beta}$$

for any  $\alpha, \beta$  fulfilling  $\alpha + \beta > 1$  and  $\alpha \in (0, 1)$ .

Using again the functional calculus with continuous functions on spectrum, for the strictly positive operator  $A$ , we have the relations (2) and (3) of the statement.

**Proposition 2.2** *Let  $X, Y$  be two strictly positive operators on  $\mathcal{H}$ , then there is  $r > 0$  having the properties  $(1 - r)I \leq X, Y \leq (1 + r)I$ , such that for any  $\alpha, \beta \in \mathbf{R}$   $\alpha + \beta > 1$  and  $\alpha \in (0, 1)$ , it is true that*

$$\alpha X + \beta Y + (\alpha + \beta)I \geq X^{\frac{\alpha}{2}} Y^{\frac{\beta}{2}} + Y^{\frac{\beta}{2}} X^{\frac{\alpha}{2}}. \quad (4)$$

*Proof.* We know by Theorem 2.1 (a) ([10]) that there is  $r > 0$ , such that

$$\alpha x + \beta y \geq x^\alpha y^\beta$$

for any  $x, y \in [1 - r, 1 + r]$ , when  $\alpha + \beta > 1$  and  $\alpha \in (0, 1)$ ,

In particular, for  $x = 1$ , it results that

$$\alpha + \beta y \geq y^\beta$$

and for  $y = 1$ , it results that

$$\alpha x + \beta \geq x^\alpha$$

in the same mentioned conditions.

Using now the functional calculus with continuous functions on the spectrum we will respectively find

$$\alpha I + \beta Y \geq Y^\beta$$

and

$$\alpha X + \beta I \geq X^\alpha.$$

Then

$$\alpha X + \beta Y + (\alpha + \beta)I \geq X^\alpha + Y^\beta \quad (5)$$

For any strictly positive operators  $U, V$  it is known that  $(U - V)^2 \geq 0$ , hence  $U^2 + V^2 \geq UV + VU$ .

By that result applied in (5) taking  $U = X^{\frac{\alpha}{2}}$  and  $V = Y^{\frac{\beta}{2}}$  it results the desired inequality (4) of the statement.

**Corollary 2.3** *In particular, if  $X = B^{-\frac{1}{2}}AB^{-\frac{1}{2}}$ ,  $Y = B^{-\frac{1}{2}}CB^{-\frac{1}{2}}$ , ( where  $A, B, C$  are strictly positive operators) check the hypothesis of Proposition 2.2 then*

$$\begin{aligned} & \alpha A + \beta C + (\alpha + \beta)B > \\ & > B^{\frac{1}{2}} \left( B^{-\frac{1}{2}}AB^{-\frac{1}{2}} \right)^{\frac{\alpha}{2}} \left( B^{-\frac{1}{2}}CB^{-\frac{1}{2}} \right)^{\frac{\beta}{2}} B^{\frac{1}{2}} + B^{\frac{1}{2}} \left( B^{-\frac{1}{2}}CB^{-\frac{1}{2}} \right)^{\frac{\beta}{2}} \left( B^{-\frac{1}{2}}AB^{-\frac{1}{2}} \right)^{\frac{\alpha}{2}} B^{\frac{1}{2}}. \end{aligned}$$

## References

- [1] Davidson K. R., *C\*-Algebras by example*, AMS, Providence, Rhode Island, (1996).
- [2] Dragomir, S., S., A survey of Jessen's type inequalities for positive functionals, *RGMA Res. Rep. Coll.*, 46 pp, (2011).
- [3] Dragomir S. S., Some new reverses of Young's operator inequality, *RGMA Res. Rep. Coll.*, 12 pp., (2015).
- [4] Dragomir S. S., Some new reverses of Young's operator inequality, *RGMA Res. Rep. Coll.*, 12 pp, (2015).
- [5] Furuichi S., On refined Young inequalities and reverse inequalities, *Journal of Mathematical Inequalities*, **5**, 1 21-31 (2011).
- [6] Furuichi S., Minculete, N., Alternative reverse inequalities for Young's inequality, *Journal of Mathematical inequalities*, **5**, 4 (2011), 595-600.
- [7] Kittaneh, F., Manasrah, Y., Reverse Young and Heinz inequalities for matrices, *Linear and Multilinear Algebra*, **59**, 9 (2011), 1031-1037.
- [8] Kittaneh, F., Manasrah, Y., Improved Young and Heinz inequalities for matrices, *J. Math. Anal. Appl.*, **361** (2010), 262-269.
- [9] Kubo F., Ando T., Means of positive operators, *Math. Ann.* 264, 209-224 (1980).

- [10] Lugojan S., Ciurdariu L., A generalization of Young's theorem and some applications, *Bull. St. al UPT*, **63** (77), Issue 2, (2018).
- [11] Young, W. H., On classes of summable functions and their Fourier series, *Proc. Royal Soc. London, Ser. A.* 87:225-229, (1912).

Loredana Ciurdariu and Sorin Lugojan  
Department of Mathematics,  
Politehnica University of Timisoara,  
P-ta. Victoriei 2, 300006, Timisoara, ROMANIA  
E-mail: loredana.ciurdariu@upt.ro  
E-mail: sorin.lugojan@upt.ro

## SOME CONCEPTS OF FRACTIONAL DIFFERENTIAL CALCULUS USING MATLAB

Elena VASILACHE

### Abstract

In the last years researches in fractional calculus was extended in many areas. For further study of its applications in Machanical Area this paper presents numerical methods for solving some differential fractional equations using MATLAB. This work contains methods for fractional calculus computations like “Grünwald-Letnikov method” or “Podlubny’s matrix approach” and examples using MATLAB for solving ordinary fractional differential equations.

<sup>1</sup>

Keywords and phrases: *fractional calculus, MATLAB, differential fractional equations, Grünwald-Letnikov*

## 1 Introduction

In the past few years, fractional computation has become a field of study that has been searched for, in the sense of applying to different branches of science [13] such as:

- Fractals [2]
- Propagation of ultrasonic waves [8, 21]
- The theory of viscoelasticity [22]
- Fluid Mechanics [12]

The concept of fractional computation appeared in 1965 and L’Hospital wrote to Leibnitz asking him the meaning of the derivative  $\frac{d^n y}{dx^n}$  if  $n = \frac{1}{2}$ . But if  $n$  were fractional, irrational or complex?

Leibnitz replied:

---

<sup>1</sup>MSC (2010): 34A08; 35R11; 65K15

If  $n = \frac{1}{2}$  then

$$d^{\frac{1}{2}}x = x\sqrt{dx} : x \quad (1.1)$$

and “a seeming paradox from which one day will draw very useful consequences”. Thus, the name of fractional computation has become an improper term for integration and arbitrary differentials.

In 1812 Laplace defined the arbitrary fractional derivatives as they were published in the writings of Lacroix’s 1819.

Starting from  $y = x^m$ ,  $m \in \mathbb{Z}_+$  Lacroix has developed the following  $n - th$  derivative:

$$\frac{d^n y}{dx^n} = \frac{m!}{(m-n)!} x^{m-n}, \quad m \geq n \quad (1.2)$$

Using the Legendre symbol for factorial, Gamma Function, (see Remark 1.1) will get:

$$\frac{d^n y}{dx^n} = \frac{\Gamma(m+1)}{\Gamma(m-n+1)} x^{m-n} \quad (1.3)$$

If  $y = x$  și  $n = \frac{1}{2}$  we have:

$$\frac{d^{\frac{1}{2}}y}{dx^{\frac{1}{2}}} = \frac{2\sqrt{x}}{\sqrt{\pi}} \quad (1.4)$$

**Remark 1.1. Definition of the Gamma function**

The most important function of fractional calculation is the Function  $\Gamma(z)$  as it is presented in [16]. It generalizes  $n!$  and allows number  $n$  to take different values of whole numbers even complex.

**Definition 1.2.** The function  $\Gamma(z)$  is defined by means of the integral:

$$\Gamma(z) = \int_0^{\infty} e^{-t} t^{z-1} dt,$$

which converges to the right half of the Complex  $Re(z) > 0$ .

Indeed, we have

$$\begin{aligned} \Gamma(x+iy) &= \int_0^{\infty} e^{-t} t^{x-1+iy} dt \\ &= \int_0^{\infty} e^{-t} t^{x-1} e^{iy \log(t)} dt \\ &= \int_0^{\infty} e^{-t} t^{x-1} [\cos(y \log(t)) + i \sin(y \log(t))] dt. \end{aligned} \quad (1.5)$$

The expression in square brackets is bordered fo  $\forall t$ . Convergence to infinity is given by  $t = 0$  we have  $x = Re(z) > 1$ .

We use (1.3) to evaluate the fractional derivative of  $f(t) = e^t$ .

$$f(t) = e^t = \sum_{k=0}^{\infty} \frac{t^k}{k!} \quad (\text{series}) \quad (1.6)$$

Applying (1.3) we obtain:

$$\frac{d^\nu}{dt^\nu} = \sum_{k=0}^{\infty} \frac{t^{k-\nu}}{\Gamma(k-\nu+1)}$$

where  $\nu > 0$  and  $\nu \in \mathbb{R}$  (real number) Fractional derivative of exponential function does not returns exponential function.

## 2 Definitions for fractional calculation

This section introduces the main definitions for fractional calculation applied in the analysis.

**Definition 2.1.** *Euler (1730)*

$$\begin{aligned} \frac{d^n x^m}{dx^n} &= m(m-1)(m-2)\dots(m-n+1)x^{m-n} \\ \Gamma(m+1) &= m(m-1)\dots(m-n+1)\Gamma(m-n+1) \\ \frac{d^n x^m}{dx^n} &= \frac{\Gamma(m+1)}{\Gamma(m-n+1)} x^{m-n} \\ \frac{d^{1/2} x}{dx^{1/2}} &= \sqrt{\frac{4x}{\pi}} = \frac{2}{\pi} x^{1/2}, \end{aligned}$$

unde  $\Gamma(z) = \int_0^{\infty} e^{-t} t^{z-1} dt$ ,  $Re(z) > 0$ .

**Definition 2.2.** *J. B. J. Fourier (1820-1822) introduced:*

$$f(x) = \frac{1}{2\pi} \int_{-\infty}^{\infty} f(z) dz \int_{-\infty}^{\infty} \cos(px - pz) dp.$$

The definition of fractional operation was obtained from the representation of the integral  $f(x)$ .

For  $n$  integer number, we have

$$\frac{d^n}{dx^n} \cos p(x-z) = p^n \cos[p(x-z) + \frac{1}{2}n\pi],$$

meaning

$$\frac{d^n f(x)}{dx^n} = \frac{1}{2\pi} \int_{-\infty}^{\infty} f(z) dz \int_{-\infty}^{\infty} p^n \cos[p(x-z) + n\frac{\pi}{2}] dp.$$

**Definition 2.3.** *N. H. Abel (1823-1826) introduced the definition of fractional integrals:*

$$\int_0^x \frac{S'(\eta)d\eta}{(x-\eta)^\alpha} = \psi(x).$$

In fact he has solved the whole for an arbitrary number  $\alpha$  and not just for  $\alpha = \frac{1}{2}$  obtaining:

$$S(x) = \frac{\sin(\pi\alpha)}{\pi} x^\alpha \int_0^1 \frac{\psi(xt)}{(1-t)^{1-\alpha}} dt.$$

After which Abel expressed the resulting solution with the help of the  $\alpha$ . order:

$$S(x) = \frac{1}{\Gamma(1-\alpha)} \frac{d^{-\alpha}\psi(x)}{dx^{-\alpha}}.$$

Abel applied the fractional calculation in the solution of the integral equation of the formulation the problem of finding the shape of the curve so that the time of frictionless descent, sliding under the action of gravity independent of the point starting. If the slip time is constantly known ( $T$ ), the equation becomes:

$$k = \int_0^x (x-t)^{-1/2} f(t) dt.$$

This equation, except  $\frac{1}{\Gamma(1/2)}$ , is the particular case of the defined integrability represents the first fraction integral  $\frac{1}{2}$ .

$$\sqrt{\pi}[d^{-1/2}/dx^{-1/2}]f(x)$$

$d^{1/2}/dx^{1/2}$ , we get

$$\frac{d^{1/2}}{dx^{1/2}}k = \sqrt{\pi}f(x).$$

**Definition 2.4.** *J. Liouville (1823-1855):*

I. In its first definition, according to the exponential representation of the function  $f(x) = \sum_{n=0}^{\infty} c_n e^{a_n x}$ , generalized the formula  $\frac{d^m e^{ax}}{dx^m} = a^m e^{ax}$  like

$$\frac{d^\nu f(x)}{dx^\nu} = \sum_{n=0}^{\infty} c_n a_n^\nu e^{a_n x}$$

II. The second type of definition was that of the fractional integral:

$$\int^\mu \Phi(x) dx^\mu = \frac{1}{(-1)^\mu \Gamma(\mu)} \int_0^\infty \Phi(x + \alpha) \alpha^{\mu-1} d\alpha$$

$$\int^\mu \Phi(x) dx^\mu = \frac{1}{\Gamma(\mu)} \int_0^\infty \Phi(x - \alpha) \alpha^{\mu-1} d\alpha$$

Substituting  $\tau = x + \alpha$  și  $\tau = x - \alpha$  in the formulas above, obtain:

$$\int^\mu \Phi(x) dx^\mu = \frac{1}{(-1)^\mu \Gamma(\mu)} \int_x^\infty (\tau - x)^{\mu-1} \Phi(\tau) d\tau$$

$$\int^\mu \Phi(x) dx^\mu = \frac{1}{\Gamma(\mu)} \int_{-\infty}^x (x - \tau)^{\mu-1} \Phi(\tau) d\tau.$$

III. The third definition, introduced the fractional derivative:

$$\frac{d^\mu F(x)}{dx^\mu} = \frac{(-1)^\mu}{h^\mu} \left( F(x) \frac{\mu}{1} F(x+h) + \frac{\mu(\mu-1)}{1 \cdot 2} F(x+2h) - \dots \right)$$

$$\frac{d^\mu F(x)}{dx^\mu} = \frac{1}{h^\mu} \left( F(x) \frac{\mu}{1} F(x-h) + \frac{\mu(\mu-1)}{1 \cdot 2} F(x-2h) - \dots \right)$$

**Definition 2.5.** *G. F. B. Riemann (1847-1876):*

Its definition for fractional integrals is:

$$D^{-\nu} f(x) = \frac{1}{\Gamma(\nu)} \int_c^x (x-t)^{\nu-1} f(t) dt + \psi(t)$$

**Definition 2.6.** *N. Ya. Sonin (1869), A. V. Letnikov (1872), H. Laurent (1884), N. Nekrasove (1888), K. Nishimoto (1987):*

*They considered the integral Cauchy formula*

$$f^{(n)}(z) = \frac{n!}{2\pi i} \int_c \frac{f(t)}{(t-z)^{n+1}} dt$$

*and replace  $n$  cu  $\nu$  got*

$$D^\nu f(z) = \frac{\Gamma(\nu+1)}{2\pi i} \int_c^{x^+} \frac{f(t)}{(t-z)^{\nu+1}} dt.$$

**Definition 2.7.** *Definition Riemann-Liouwill:*

*The classic definition of fractional calculation is the one that shows the link between the two previous definitions.*

$${}_a D_t^\alpha f(t) = \frac{1}{\Gamma(n-\alpha)} \left( \frac{d}{dt} \right)^n \int_a^t \frac{f(\tau) d\tau}{(t-\tau)^{\alpha-n+1}}$$

$$(n-1 \leq \alpha < n)$$

**Definition 2.8.** *Grünwald-Letnikove:*

*This is another definition that is sometimes useful.*

$${}_a D_t^\alpha f(t) = \lim_{h \rightarrow 0} h^{-\alpha} \sum_{j=0}^{\lfloor \frac{t-a}{h} \rfloor} (-1)^j \binom{\alpha}{j} f(t-jh)$$

**Definition 2.9.** *M. Caputo (1967):*

*The second common definition is*

$${}_a^C D_t^\alpha f(t) = \frac{1}{\Gamma(\alpha-n)} \int_a^t \frac{f^{(n)}(\tau) d\tau}{(t-\tau)^{\alpha+1-n}}$$

$$(n-1 \leq \alpha < n)$$

**Definition 2.10.** *Oldham and Spanier (1974):*

$$\frac{d^q f(\beta x)}{dx^q} = \beta^q \frac{d^q f(\beta x)}{d(\beta x)^q}$$

**Definition 2.11.** *K. S. Miller, B. Ross (1993):*

*They used a different operator  $D$  as*

$$D^{\bar{\alpha}} f(t) = D^{\alpha_1} D^{\alpha_2} \dots D^{\alpha_n} f(t), \quad \bar{\alpha} = (\alpha_1, \alpha_2, \dots, \alpha_n)$$

*where  $D^{\alpha_i}$  is definition of Riemann-Liouville or Caputo.*

### 3 Fractional derivatives for some special functions

**1. Unit function:** For  $f(x) = 1$  we have

$$\frac{d^q 1}{dx^q} = \frac{x^{-q}}{\Gamma(1-q)}, \quad \forall q.$$

**2. The identical function:** For  $f(x) = x$  we have

$$\frac{d^q x}{dx^q} = \frac{x^{1-q}}{\Gamma(2-q)}.$$

**3. The exponential function:**  $f(x) = e^x$  is

$$\frac{d^q e^{\pm x}}{dx^q} = \sum_{k=0}^{\infty} \frac{x^{k-q}}{\Gamma(k-q+1)}.$$

**4. The sinus function:** If  $f(x) = \sin x$  then

$$\frac{d^q \sin(x)}{dx^q} = \sin\left(x + \frac{q\pi}{2}\right).$$

**5. The cosinus function:** If  $f(x) = \cos x$  then

$$\frac{d^q \cos(x)}{dx^q} = \cos\left(x + \frac{q\pi}{2}\right).$$

### 6. Fractional derivatives ${}_L D_+^\alpha$ according to Liouville for some functions special

$$f(x) \quad \frac{d^\alpha}{dx^\alpha} f(x)$$

$$e^{kx} \quad k^\alpha e^{kx} \quad k \geq 0$$

$$\sin(kx) \quad k^\alpha \sin(kx + \frac{\pi}{2}\alpha)$$

$$\cos(kx) \quad k^\alpha \cos(kx + \frac{\pi}{2}\alpha)$$

$$\operatorname{erf}(kx) \quad \text{divergent}$$

$$\begin{aligned} e^{-kx^2} \quad & \frac{k^{\frac{\alpha}{2}}}{\Gamma(1-\alpha)} (\Gamma(1-\frac{\alpha}{2}) {}_1F_1(\frac{1}{2} + \frac{\alpha}{2}; \frac{1}{2}; -kx^2) \\ & - \sqrt{k}\alpha x \Gamma(\frac{1}{2} - \frac{\alpha}{2}) {}_1F_1(1 + \frac{\alpha}{2}; \frac{3}{2}; -kx^2)) \\ & - 2\sqrt{k}\alpha x \Gamma(\frac{3}{2} - \frac{\alpha}{2}); {}_1F_1(\frac{1}{2} + \frac{\alpha}{2}; \frac{3}{2}; -kx^2) \\ & - \frac{2}{3}k(1-\alpha^2)x^2 \Gamma(\frac{1}{2} - \frac{\alpha}{2}) {}_1F_1(\frac{3}{2} + \frac{\alpha}{2}; \frac{5}{2}; -kx^2)) \end{aligned}$$

$$\begin{aligned} {}_pF_q(\{a_i\}; \{b_j\}; kx) \quad & k^\alpha \prod_{i=1}^p \frac{\Gamma(a_i + \alpha)}{\Gamma(a_i)} \prod_{j=1}^q \frac{\Gamma(b_j)}{\Gamma(b_j + \alpha)} \\ & {}_pF_q(\{a_i + \alpha\}; \{b_j + \alpha\}; kx) \end{aligned}$$

$$|x|^{-k} \quad \frac{\Gamma(k+\alpha)}{\Gamma(k)} |x|^{-k-\alpha}, \quad x < 0$$

### 7. Several special functions and their fractional derivatives ${}_R D^\alpha$ according to the Riemann definition

$$f(x) \quad \frac{d^\alpha}{dx^\alpha} f(x)$$

$$e^{kx} \quad \operatorname{sign}(x)(\operatorname{sign}(x)k)^\alpha$$

$$\begin{aligned}
& e^{kx} \left( 1 - \frac{\Gamma(-\alpha, kx)}{\Gamma(-\alpha)} \right) \\
\sin(kx) & \quad \frac{(2-\alpha) k \operatorname{sign}(x) |x|^{-\alpha}}{(2-3\alpha+\alpha^2)\Gamma(1-\alpha)} {}_1F_2 \left( 1; \frac{3}{2} - \frac{\alpha}{2}, 2 - \frac{\alpha}{2}; -\frac{1}{4}k^2x^2 \right) \\
& \quad - \frac{k^3 \operatorname{sign}(x) |x|^{-\alpha} x^3}{\left(\frac{3}{2}-\frac{\alpha}{2}\right)\left(2-\frac{\alpha}{2}\right)(2-3\alpha+\alpha^2)\Gamma(1-\alpha)} {}_1F_2 \left( 2; \frac{5}{2} - \frac{\alpha}{2}, 3 - \frac{\alpha}{2}; -\frac{1}{4}k^2x^2 \right) \\
\cos(kx) & \quad \frac{\operatorname{sign}(x) |x|^{-\alpha}}{\Gamma(4-\alpha)} \\
& \quad \left( (\alpha-1)(\alpha-2)(\alpha-3) {}_1F_2 \left( 1; 1 - \frac{\alpha}{2}, \frac{3}{2} - \frac{\alpha}{2}; -\frac{1}{4}k^2x^2 \right) \right. \\
& \quad \left. + 2k^2x^2 {}_1F_2 \left( 2; 2 - \frac{\alpha}{2}, \frac{5}{2} - \frac{\alpha}{2}; -\frac{1}{4}k^2x^2 \right) \right) \\
\operatorname{erf}(kx) & \quad - 2^{-1+\alpha} k \operatorname{sign}(x) |x|^{-\alpha} \\
& \quad \left( (\alpha-2) {}_2\bar{F}_2 \left( \frac{1}{2}, 1; \frac{3}{2} - \frac{\alpha}{2}, 2 - \frac{\alpha}{2}; -k^2x^2 \right) \right. \\
& \quad \left. + k^2x^2 {}_2\bar{F}_2 \left( \frac{3}{2}, 2; \frac{5}{2} - \frac{\alpha}{2}, 3 - \frac{\alpha}{2}; -k^2x^2 \right) \right) \\
{}_pF_q(\{a_i\}; \{b_j\}; kx) & \quad \frac{\operatorname{sign}(x) |x|^{-\alpha}}{\Gamma(1-\alpha)^{p+1}} F_{q+1}(\{1, 1 + a_i\}; \{b_j, 2 - \alpha\}; kx) \\
& \quad + k \operatorname{sign}(x) |x|^{-\alpha} x^{1-(1-\alpha)(2-\alpha)\Gamma(1-\alpha)} \prod_{i=1}^p a_i \prod_{j=1}^q \frac{1}{b_j} \\
& \quad \times {}_{p+1}F_{q+1}(\{2, 1 + a_i\}; \{1 + b_j, 3 - \alpha\}; kx) \\
\log(x) & \quad \frac{x^{-\alpha}}{\Gamma(2-\alpha)} (1 - (1-\alpha)(H_{1-\alpha} + \log(x))), \quad x > 0 \\
x^k & \quad \frac{\Gamma(1+k)}{\Gamma(1+k-\alpha)} \operatorname{sign}(x) |x|^{-\alpha} x^k
\end{aligned}$$

## 4 Method Grünwald-Letnikov

For the numerical calculation of the fractional derivatives we can use the relation:

$$({}^{k-L_m/h}D_{t_k}^q f(t) \approx h^{-q} \sum_{j=0}^k (-1)^j \binom{q}{j} f(t_{k-j}) = h^{-q} \sum_{j=0}^k c_j^{(q)} f(t_{k-j}) \quad (4.1)$$

resulting from the Grünwald-Letnikov relation in Definition 2.8.

This approach is based on the fact that for most of the function classes, the definitions of Grünwald-Letnikov, Riemann-Liouville and M. Caputo are equivalent if  $f(a) = 0$ .

Relationship for the explicit numerical approximation of the  $q$ -derivative in the points  $kh, (k = 1, 2, \dots)$  has the above given form (see 4.1) (Dorčák, 1994; Podlubny, 1999), where:

–  $L_n$  is memory length

–  $t_k = kh$

–  $h$  = the time at that step

–  $c_j^{(q)} (j = 0, 1, \dots, k)$  = coefficient binomial.

To calculate them, we can use mathematical relations:

$$c_0^{(q)} = 1, \quad c_j^{(q)} = \left(1 - \frac{1+q}{j}\right) c_{j-1}^{(q)}. \quad (4.2)$$

Binomial coefficients  $c_j^{(q)} (j = 0, 1, \dots, k)$  can also be expressed factorial. By factorial writing, *Function Gamma* allows us to generalize the binomial coefficients for arguments that are not integers.

$$(-1)^j \binom{q}{j} = (-1)^j \frac{\Gamma(q+1)}{\Gamma(j+1)\Gamma(q-j+1)} = \frac{\Gamma(j-q)}{\Gamma(-q)\Gamma(j+1)}. \quad (4.3)$$

Obviously, for this simplification, the accuracy of the result is lost.

If  $f(t) < M$ , we can very easily set the estimated  $L_m$  (with accuracy  $\epsilon$ )

$$L_m \geq \left(\frac{M}{\epsilon|\Gamma(1-q)|}\right)^{\frac{1}{q}}. \quad (4.4)$$

This is called Power Series Expansion (PSE). Transfer function discretely resulting, the approximate fractional order operators can be expressed in the range  $-z$  in the following way:

$${}_0D_{kT}^{\pm r} G(z) = \frac{Y(z)}{F(z)} = \left(\frac{1}{T}\right)^{\pm r} PSE \{(1 - z^{-1})^{\pm r}\}_n \approx T^{\mp r} R_n(z^{-1}), \quad (4.5)$$

where:

- $T$  – reference;
- $PSE\{u\}$  – The function results from the application of the PSE function  $u$ ;
- $Y(z)$  is converted "Z" of the output sequence  $y(kT)$ ;
- $F(z)$  is converted "Z" of the input sequence  $f(kT)$ ;
- $n$  – the order of approximation;
- $R$  – the n-polynom in variable  $z^{-1}$  and  $k = 1, 2, \dots$

**Application 4.1.** Let the order of fractional derivation  $\alpha \in [0, 1]$  for the function  $y = \sin(t)$  with  $t \in [0, 2\pi]$ . The following code in MATLAB uses the command `fderiv()` entered by Bayat (2007) and based on 4.1.

Input data:

```
clear all; close all;
h = 0.01; t = 0 : h : 2 * pi;
y = sin(t);
order = 0 : 0.1 : 1;
for i = 1 : length (order)
    yd(i, :) = fderiv(order(i), y, h);
end
[X, Y] = meshgrid (t, order);
mesh (X, Y, yd)
xlabel (t'); ylabel ('\alpha'); zlabel ('y')
```

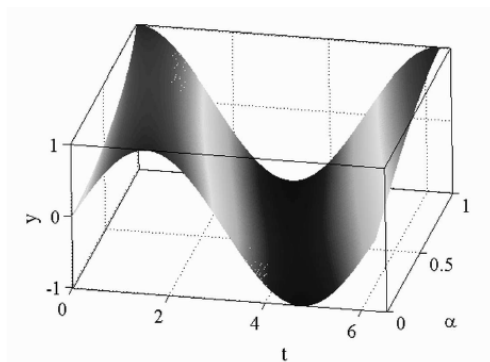


Figure 1: Fractional derivative of function  $y = \sin(t)$

Figure 1 is a graphical derivative of the sinus function for fractional derivation order  $0 < \alpha < 1$  and  $0 < t < 2\pi$ .

**Aplication 4.2.** We can get a better approximation of the fractional derivative if  $h$  of the first relation  $h$  is small enough so it can be demonstrated that the accuracy of this methods is 0. The MATLAB code for the application function 4.1 and the function  $e^x$ .

Input:

```
function dy =gdiff(y, x, gam)
h = x(2) - x(1); dy(1) = 0; y = y(:); x = x(:);
w = 1;
for j = 2 : length(x), w(j) = w(j - 1)*(1 - (gam + 1)/(j - 1));
end
for i = 2 : length(x), dy(i) = w(1 : i)*[y(i : -1 : 1)]/h^gam;
end
by Matlab code
t = 0 : 0.001 : pi; y = sin(t); dy = gdiff(y, t, 0.9); plot(t, dy)
t = 0 : 0.001 : pi; y = sin(t); dy = gdiff(y, t, 0.9); plot(t, dy);
hold on;
t = 0 : 0.001 : pi; y = sin(t); dy = gdiff(y, t, 0.1); plot(t, dy);
t = 0 : 0.001 : pi; y = sin(t); dy = gdiff(y, t, 0.5); plot(t, dy);
```

we get 0.1, 0.5 a 0.9 derivative of function  $\sin(x)$  see the fig below:

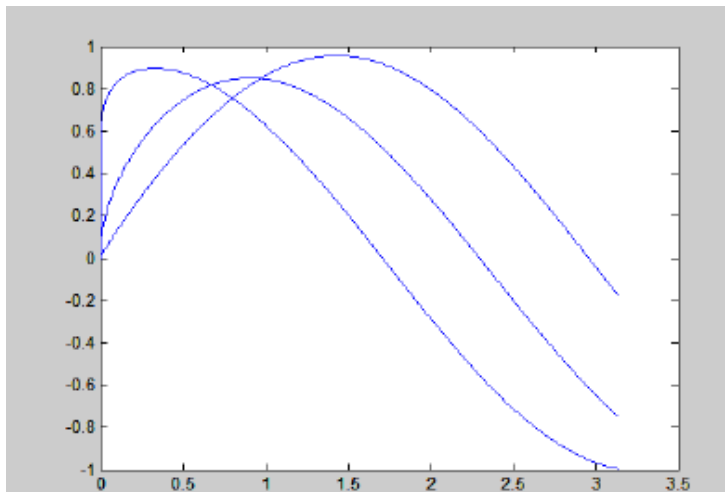


Figure 2: The 0.1, 0.5, 0.9 derivative of function  $\sin(x)$

By Matlab:

```
t = 0 : 0.001 : 3; y = exp(t); plot(t, y)
t = 0 : 0.001 : 3; y = exp(t); plot(t, y)
hold on;
t = 0 : 0.001 : 3; y = exp(t); dy = gdiff(y, t, 0.3); plot(t, dy)
t = 0 : 0.001 : 3; y = exp(t); dy = gdiff(y, t, 0.5); plot(t, dy)
t = 0 : 0.001 : 3; y = exp(t); dy = gdiff(y, t, 0.7); plot(t, dy)
```

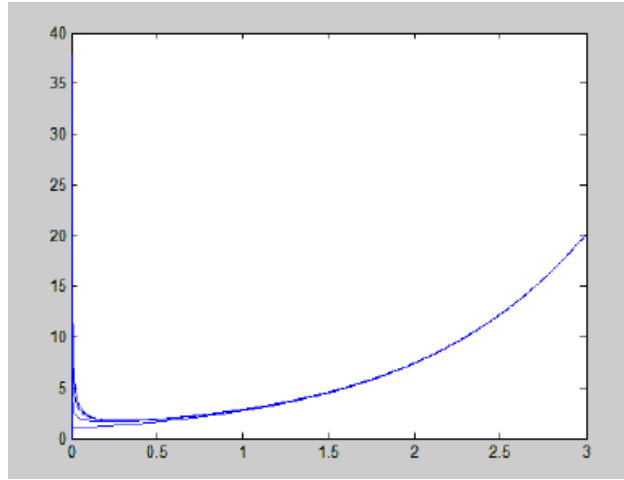


Figure 3: The 0.3, 0.5, 0.7 derivative of function  $e^x$

It is observed in figurative representation how 0.3–a 0.5-a și 0.7 – a derivatives of  $e^x$  are almost identical, which is similar to the classical derivation so  $(e^z)' = e^z$  and  $e^z \alpha$  derivativetimes that is also maintained for  $\alpha$  =fractional.

## 5 Differential fractional equations

The general fractional system can be described by means of the differential equation fractional form:

$$a_n D_t^{\alpha_n} y(t) + a_{n-1} D_t^{\alpha_{n-1}} y(t) + \dots + a_0 D_t^{\alpha_0} y(t) = b_m D_t^{\beta_m} u(t) + b_{m-1} D_t^{\beta_{m-1}} u(t) + \dots + b_0 D_t^{\beta_0} u(t), \quad (5.1)$$

where  $D_t^\gamma \equiv {}_0 D_t^\gamma$  express Grünwald-Letnikov, Riemann-Liouville sau Caputo derivatives fractional. The corresponding irrational transfer function has the form

$$G(s) = \frac{b_m s^{\beta_m} + \dots + b_1 s^{\beta_1} + b_0 s^{\beta_0}}{a_n s^{\alpha_n} + \dots + a_1 s^{\alpha_1} + a_0 s^{\alpha_0}} = \frac{Q(s^{\beta_k})}{P(s^{\alpha_k})}, \quad (5.2)$$

where  $a_k (k = 0, \dots, n)$ ,  $b_k (k = 0, \dots, m)$  are constants, and  $\alpha_k (k = 0, \dots, n)$ ,  $\beta_k (k = 0, \dots, m)$  are real or rational numbers of any kind and without limitation the generality may be arranged

$$\alpha_n > \alpha_{n-1} > \dots > \alpha_0, \quad \beta_m > \beta_{m-1} > \dots > \beta_0. \quad (5.3)$$

In a particular case for systems of commensurable order, keep  $\alpha_k = \alpha k$ ,  $\beta_k = \alpha k$ , ( $0 < \alpha < 1$ ),  $\forall k \in \mathbb{Z}$ , and the transfer function has the following form:

$$G(s) = K_0 \frac{\sum_{k=0}^M b_k (s^\alpha)^k}{\sum_{k=0}^N a_k (s^\alpha)^k} = K_0 \frac{Q(s^\alpha)}{P(s^\alpha)}. \quad (5.4)$$

With  $N > M$ , the function  $G(s)$  becomes its own rational function in complex variables  $s^\alpha$  and what can be extended to form:

$$G(s) = K_0 \left[ \sum_{i=1}^N \frac{A_i}{s^\alpha + \lambda_i} \right],$$

where  $\lambda_i (i = 1, 2, \dots, N)$  are the roots of the pseudo polynomial or the polynomial system. The analytical solution of the system can be expressed

$$y(t) = \mathcal{L}^{-1} \left\{ K_0 \left[ \sum_{i=1}^N \frac{A_i}{s^\alpha + \lambda_i} \right] \right\} = K_0 \sum_{i=1}^N A_i t^\alpha E_{\alpha, \alpha}(-\lambda_i t^\alpha), \quad (5.5)$$

$$a_n D_t^{\alpha n} y(t) + \dots + a_1 D_t^{\alpha 1} y(t) + \dots + a_0 D_t^{\alpha 0} y(t) = 0, \quad (5.6)$$

where  $a_k (k = 0, 1, \dots, n)$  are constant coefficients;  $\alpha_k (k = 0, 1, 2, \dots, n)$  are real numbers.

Without restricting generality, we can assume that  $\alpha_n > \alpha_{n-1} > \dots > \alpha_0 \geq 0$ .

The analytical solution of 5.6 is given by the general formula in the form:

$$y(t) = \frac{1}{a_n} \sum_{m=0}^{\infty} \frac{(-1)^m}{m!} \sum_{\substack{k_0+k_1+\dots+k_{n-2}=m \\ k_0 \geq 0, \dots, k_{n-2} \geq 0}} (m; k_0, k_1, \dots, k_{n-2}) \\ \times \prod_{i=0}^{n-2} \left( \frac{a_i}{a_n} \right)^{k_i} \mathcal{E}_m \left( t, -\frac{a_{n-1}}{a_n}; \alpha_n - \alpha_{n-1}, \alpha_n + \sum_{j=0}^{n-2} (\alpha_{n-1} - \alpha_j) k_j + 1 \right),$$

where  $(m, k_0, k_1, \dots, k_{n-2})$  are multinomial coefficients.

It is the control function that modifies the system 5.6 in:

$$a_n D_t^{\alpha_n} y(t) + \dots + a_1 D_t^{\alpha_1} y(t) + a_0 D_t^{\alpha_0} y(t) = u(t). \quad (5.7)$$

Through Laplace, we get the fractional transfer function:

$$G(s) = \frac{Y(s)}{U(s)} = \frac{1}{a_n s^{\alpha_n} + \dots + a_1 s^{\alpha_1} + a_0 s^{\alpha_0}}. \quad (5.8)$$

**Application 5.1.** Given a fractional differential of the second order, with initial zero conditions,  $\alpha = 1.5, a = 2, b = 1, \text{pasul} = 0.001$  calculation time 20sec. :

$$a D_t^\alpha y(t) + b y(t) = 1. \quad (5.9)$$

The solution can be obtained using Laplace's transformation method, it can be expressed:

$$Y(s) = \frac{1/a}{s(s^\alpha + b/a)} \quad (5.10)$$

and the general solution is as follows:

$$y(t) = \frac{1}{a} \mathcal{E}_0(t, -\frac{b}{a}; \alpha, \alpha + 1) \equiv \frac{1}{a} t^\alpha E_{\alpha, \alpha+1} \left( -\frac{b}{a} t^\alpha \right). \quad (5.11)$$

To get the solution in MATLAB, we can use the following commands:

```
clear all; close all;
a = 2; b = 1; alpha = 1.5;
t = 0 : 0.001 : 20;
y = (1/a) * t.^(alpha) * mlf(alpha, alpha + 1, ((-b/a) * t.^(alpha)));
plot(t, y);
xlabel('Time[sec]');
ylabel('y(t)');
```

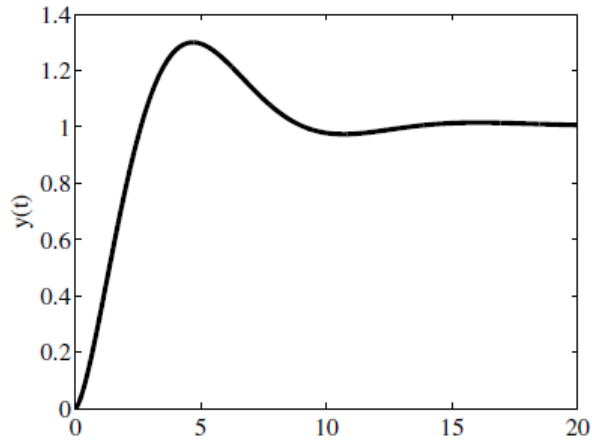


Figure 4: The equation solution

## References

- [1] F. Barpi, S. Valente, *Creep and fracture in concrete: a fractional order rate approach*, Elsevier Science Ltd. (2002);
- [2] A. Carpinteri, B. Chiaia, P. Cornetti, *A fractional calculus approach to the mechanics of fractal media*, Volume 58, Torino (2000);
- [3] A. Carpinteri, Kiran, M. Kolwankar, P. Cornetti, *Calculation of the tensile and flexural strength of disordered materials using fractional calculus*, Elsevier Ltd. (2004);
- [4] A. Carpinteri, P. Cornetti, F. Barpi, S. Valente, *Cohesive crack model description of ductile to brittle size-scale transition: dimensional analysis vs. renormalization group theory*, Elsevier Science Ltd. (2003);
- [5] C. G. Koh, J. M. Kelly, *Application of Fractional Derivatives to Seismic Analysis of Base-Isolated Models*, Volume 19, Page 229-241 (1990);
- [6] C. Chi, F. Gao, *Simulating Fractional Derivatives using Matlab*, Journal of Software, Volume 8, Number 3, (March 2013);
- [7] D. Valério, J. T. Machado, V. Kiryakova, *Some pioneers of the applications of fractional calculus*, Volume 17, Number 2 (2014);

- [8] Z. E. A. Fellah, C. Depollier, *Application of fractional calculus to the sound waves propagation in rigid porous materials: Validation via ultrasonic measurement*, Acta Acustica vol.88 (2002) 34-39;
- [9] I. Podlubny, *Matrix approach to discrete fractional calculus*, Volume 3, Number 4 (2000);
- [10] I. Podlubny, *Fractional differential equations*, Mathematics in sciences and engineering, Volume 198;
- [11] I. Petráš, *An Effective Numerical Method and Its Utilization to Solution of Fractional Models Used in Bioengineering Applications*, Hindawi Publishing Corporation (2011);
- [12] I. Petráš, *Fractional Derivatives, Fractional Integrals and Fractional Differential Equations in MATLAB*, Intech (2011);
- [13] V. V. Kulish, J. L. Large, *Application of Fractional Calculus to Fluid Mechanics*, J. Fluids Eng.-September 2002 - Volume 124, Issue 3, 803 (4 pages);
- [14] L. Debnath, *Recent Applications of Fractional Calculus to Science and Engineering*, Hindawi Publishing Corporation (2003);
- [15] M. Dalir, M. Bashour, *Applications of Fractional Calculus*, Applied Mathematical Sciences, Volume 4, Number 21, Page 1021-1032 (2010);
- [16] I. Podlubny, *Mathematics in Science and Engineering*, Academic Press, USA (1999);
- [17] R. Herrmann, *Fractional Calculus an Introduction for Physicists*, World Scientific (2011);
- [18] R. Herrmann, *Fractional Calculus*, [www.worldscientific.com](http://www.worldscientific.com).
- [19] J. Sabatier, O. P. Agrawal, J. A. T. Machado, *Theoretical Developments and Applications in Physics and Engineering*, Springer (2007);
- [20] S. Townsend, *Numerical Methods in Fractional Calculus*, Department of Mathematics and Statistics (2015);
- [21] N. Sebaa, Z. E. A. Fellah, W. Lauriks, C. Depollier, *Application of fractional calculus to ultrasonic wave propagation in human cancellous bone*, Signal Processing archive Volume 86, Issue 10(2006) 2668-2677;

- [22] E. Soczkiewicz, *Application of fractional calculus in the theory of viscoelasticity*, Molecular and Quantum Acoustics Vol. 23, 397-404(2002);
- [23] J. T. Machado, F. Mainardi, V. Kiryakova, *Fractional calculus: Quo vadimus? (Where are we going?)*, Volume 18, Number 2 (2015);
- [24] J. T. Machado, V. Kiryakova, F. Mainardi, *A poster about the recent history of fractional calculus*, Volume 13, Number 3 (2010);
- [25] J. T. Machado, A. M. Galbano, J. J. Trujillo, *Science metrics on fractional calculus development since 1966*, Volume 16, Number 2 (2013);
- [26] V. Kiryakova, *An International Journal for Theory and Applications*, Sofia, Bulgaria (2002);
- [27] X.-J. Yang, *Advanced Local Fractional Calculus and Its*, World Science Publisher (2012).

Elena Vasilache  
Department of Mathematics,  
"Ovidius" University of Constanța,  
Ion Voda 58, 900573, Constanța, ROMANIA  
E-mail: elena\_lmm@yahoo.com

## INSTRUCTIONS FOR THE AUTHORS

The "Buletinul Științific al Universității Politehnica Timișoara" is a direct successor of the "Buletin scientifique de l'École Polytechnique de Timișoara" which was started in 1925. Between 1982 – 1989 it was published as the "Lucrările Seminarului de Matematică și Fizică ale Institutului Politehnic "Traian Vuia" din Timișoara".

Publication program: one volume per year in two issues, each series.

The "Mathematics-Physics" series of the "Buletinul Științific al Universității Politehnica Timișoara" publishes original papers in all areas of the pure and applied mathematics and physics.

1. The manuscript should be sent to the Editor, written in [English](#) (or French, or German, or Russian). The manuscript should be prepared in [LATEX](#).
2. Maximum length of the paper is 8 pages, preferably in an even number of pages, in Times New Roman (12 pt).
3. For the first page the authors must bear in view:
  - an Abstract single spaced (at most 150 words) will be placed before the beginning of the text as: ABSTRACT. The problem of ...
  - footnote with MSC (Mathematics Subjects Classification) or PACS (Physics Abstracts Classification System) Subject Classification Codes (10 pt)
4. Graphs, illustrations and tables should be placed into the manuscript (send it as .eps or .pdf file), with the corresponding consecutively number and explanations under them.
5. The complete author's (authors') address(es) will be placed after References.
6. A Copyright Transfer Agreement is required together with the paper. By submitting a paper to this journal, authors certify that the manuscript has not been submitted to, nor is it under consideration for publication by another journal, conference proceedings, or similar publications.
7. There is no page charge and after registration a paper is sent to two independent referees. After acceptance and publication the author will receive 5 reprints free of charge. If a larger amount is required (fee of 2 USD per copy per article) this should be communicated to the Editor.
8. Manuscripts should be sent to:

### For Mathematics

Dr. Liviu CĂDARIU  
POLITEHNICA UNIVERSITY TIMISOARA  
Department of Mathematics  
Victoriei Square, No. 2  
300006 – TIMIȘOARA, ROMANIA  
[liviu.cadariu-brailoiu@mat.upt.ro](mailto:liviu.cadariu-brailoiu@mat.upt.ro)

### For Physics

Dr. Dušan POPOV  
POLITEHNICA UNIVERSITY TIMISOARA  
Department of Physical Fundamentals  
of Engineering  
B-dul. V. Parvan, No.2  
300223 – TIMIȘOARA, ROMANIA  
[dusan.popov@et.upt.ro](mailto:dusan.popov@et.upt.ro)